AN ABSTRACT OF THE THESIS OF

Daniel E. Sigmon for the degree of Master of Science in Oceanography presented on June 6, 2001. Title: Production and Export of Biogenic Silica in the Southern Ocean.

Abstract approved: Redacted for privacy

David M. Nelson

Dissolved silicic acid ($Si(OH)_4$) and biogenic silica ($BSiO_2$) concentrations were measured on four different cruises in the Southern Ocean along 170° W from late October 1997 to mid-March 1998. These data were used to construct a vertically integrated Si budget in the surface layer from 58° to 68° S. Throughout that period there was a distinct, southward-moving meridional [$Si(OH)_4$] gradient, with concentrations increasing to the south. In October the gradient was centered on the Antarctic Polar Front (APF) at 61° S. Surface layer [$Si(OH)_4$] increased from 10 to >40 mmol m^{-3} between 58° and 62° S, and $BSiO_2$ concentrations were <125 mmol m^{-2} throughout the study area. As the surface mixed layer stratified and shoaled in December, diatoms bloomed in response to the more favorable light conditions, consuming $Si(OH)_4$ in the process. By late December $BSiO_2$ concentrations were exceptionally high for the open ocean, with maximum integrated values of 700 mmol Si m^{-2} around 62° S, while vertically integrated [$Si(OH)_4$] in the upper 50 m had dropped from 2,500 to 870 mmol m^{-2}, an average decrease of >30 mmol Si m^{-3}. The diatom bloom persisted into January with maximum integrated $BSiO_2$ of 600 mmol m^{-2} between 64° and 65° S, while [$Si(OH)_4$] was depleted to <2 mmol m^{-3} in surface waters as far south as 64.5° S. The center of the [$Si(OH)_4$] gradient had moved southward to 65° S by late January, coincident with maximal diatom biomass at that time. The bloom ended by March with the disappearance of most of the diatom biomass from the surface layer, deeper mixed layers, and increased [$Si(OH)_4$]. By late January, diatom production had removed >70% of the of $Si(OH)_4$ initially present in the upper 50 m everywhere north of 65° S, and had displaced the [$Si(OH)_4$] gradient >400 km southward, while the APF remained stationary. Between November and late January (~80 days), an average of 2,200 mmol Si m^{-2} had been removed from the upper 50 m between 61° and 65° S.

Based on changes in vertically integrated $Si(OH)_4$ and $BSiO_2$ concentrations between November and March, an average of 2 mol Si m^{-2} was exported from the upper 50 m between 61° and 65° S, with 59% of that export occurring between late December and late January. The observed seasonal export is very high in comparison with other oceans, and the high export coincides spatially with a well-documented zone of high opal flux to 1,000 m and high opal content in modern sediments. North of 61° S $BSiO_2$ export was limited by the low initial standing stock of $Si(OH)_4$ in surface waters and south of 65° S export was likely limited by the shorter growing season. Thus the combined effect of a large initial supply of $Si(OH)_4$ in surface waters and conditions that permit efficient use of that Si by diatoms appears to be the primary cause of opal-rich sediment accumulation in the Pacific sector of the Southern Ocean.

Production and Export of Biogenic Silica in the Southern Ocean

by
Daniel E. Sigmon

A THESIS

submitted to

Oregon State University

In partial fulfillment of
the requirements for the
degree of

Master of Science

Presented June 6, 2001
Commencement June 2002

Master of Science thesis of Daniel E. Sigmon presented on June 6, 2001

APPROVED:

Redacted for privacy

Major Professor, representing Oceanography

Redacted for privacy

Dean of the College of Oceanic and Atmospheric Sciences

Redacted for privacy

Dean of Graduate School

I understand that my thesis will become part of the permanent collection of Oregon State University libraries. My signature below authorizes release of my thesis to any reader upon request.

Redacted for privacy

Daniel E. Sigmon, Author

ACKNOWLEDGEMENTS

I would like to thank Valerie Franck, Julie Arrington, and Bill Golden for their admirable efforts to help collect samples and data for this project. I would also like to thank Mark Abbott for his support during my graduate program. I also thank the crew of the R/V Revelle for allowing us to perform our work as smoothly as possible. This work was funded by the National Science Foundation through grants OPP-9530677 and OCE-9911312 to Oregon State University and OPP-9531982 to the University of California, Santa Barbara.

CONTRIBUTION OF AUTHORS

Mark Brzezinski and David Nelson were the principal investigators for our Southern Ocean project. Both were involved with the data collection and analyses. Their considerable insight and assistance have greatly benefited not only my submitted manuscript, but my thesis as well.

TABLE OF CONTENTS

	Page
1. A SUMMARY OF THE MARINE Si CYCLE	1
2. THE Si CYCLE IN THE PACIFIC SECTOR OF THE SOUTHERN OCEAN: SEASONAL DIATOM PRODUCTION AND EXPORT TO THE DEEP SEA	8
Introduction	9
Methods	11
Results	14
Discussion	39
3. COUPLING OF THE SURFACE Si CYCLE TO Si FLUX AND BURIAL	50
BIBLIOGRAPHY	57
APPENDIX	62

LIST OF FIGURES

Figure		Page
1.	Contours of $Si(OH)_4$ concentrations along 170° W with station profiles shown (dashed line represents southern edge of APF)	15
2.	Contours of $BSiO_2$ concentrations along 170° W with station profiles shown (dashed line represents southern edge of APF)	17
3.	Integrated $Si(OH)_4$ concentrations along 170° W between 58° and 68° S	18
4.	Integrated $BSiO_2$ concentrations along 170° W between 58° and 68° S	22
5.	Regression of integrated $BSiO_2$ accumulation to $Si(OH)_4$ removal between successive cruises during which $BSiO_2$ increased and $Si(OH)_4$ decreased from 58° and 68° S. The dashed line indicates a 1:1 relationship between $BSiO_2$ accumulation and $Si(OH)_4$ removal	23
6.	Total integrated Si export from the upper 50 m and the % of initial Si this export represents	26
7.	Regression of euphotic zone depth as a function of average $BSiO_2$ concentration for all profile stations	28
8.	Regression of euphotic zone depth as a function of average chl *a* concentration for all profile stations	28
9.	Correlation of average $BSiO_2$ concentrations to average chl *a* concentrations for all profile stations	29

LIST OF TABLES

Table		Page
1.	Integrated silicic acid concentrations and changes (all in mmol m^{-2})	20
2.	Integrated biogenic silica concentrations and changes (all in mmol m^{-2})	22
3.	Total surface layer Si concentrations and changes (all in mmol m^{-2})	25
4.	Seasonal production and export of $BSiO_2$ in the region just south of the Antarctic Polar Front (in mol m^{-2})	48
5.	Comparison of Si export based on net changes in total surface layer Si, ^{234}Th fluxes, sediment trap data, and Si flux to and burial in the seabed (all in mmol m^{-2})	52

Production and Export of Biogenic Silica in the Southern Ocean

Chapter 1:

A Summary of the Marine Si Cycle

The element silicon (Si) exists in the ocean in particulate and dissolved phases. The particulate phases are lithogenic silica ($LSiO_2$), formed by physical weathering of crustal rocks, and biogenic silica ($BSiO_2$), formed by several types of marine organisms. Dissolved Si in the ocean is composed of >97% silicic acid ($Si(OH)_4$) (Stumm & Morgan 1981). The oceans contain ~10^{17} moles of $Si(OH)_4$ and have a mean concentration of ~70 μM (Tréguer et al. 1995). Silicic acid is supplied to the marine environment primarily via river inputs of Si through weathering of crustal rocks. The riverine $Si(OH)_4$ inputs of ~5 x 10^{12} moles (10^{12} = 1 teramole or Tmol) per year are >10 times any other input source (Tréguer et al. 1995). Based on total $Si(OH)_4$ inputs, the steady-state residence time for Si in the ocean is ~15,000 years. However, the cycling of Si in the oceans is controlled by biological production of $BSiO_2$ and its subsequent dissolution back to $Si(OH)_4$, which generally occurs on time scales of days to weeks. In fact ~240 Tmol yr^{-1} of $Si(OH)_4$ are converted to $BSiO_2$, predominantly by diatoms, which is ~40 times the total annual input of $Si(OH)_4$ to the marine environment (Tréguer et al. 1995). Of this $BSiO_2$ production, >95% is dissolved in the ocean and at the seafloor before burial (Nelson et al. 1995), and it is mainly this recycling of $BSiO_2$, not inputs of $Si(OH)_4$, that supports $BSiO_2$ production in the surface layer. The relatively rapid rates of $BSiO_2$ production and dissolution result in ~400 year residence time of Si in the biological cycle, implying that a molecule of $Si(OH)_4$ supplied to the marine environment is converted to $BSiO_2$ and dissolved back to $Si(OH)_4$ ~40 times before being buried and lost from the system. Therefore, the marine biogeochemical Si cycle can be thought of as a balance between $Si(OH)_4$ inputs and $BSiO_2$ burial on long time scales (>10,000 y), and between the formation and dissolution of $BSiO_2$ on shorter time scales.

All phases of Si have marked spatial variations. Suspended lithogenic silica is most abundant in continental margins due to supply of crustal minerals (especially clays) in nearshore environments, and near the seafloor due to resuspension of sedimented material. However, due to their slow rates of dissolution and near-saturation (100-200 μM; Stumm & Morgan 1981) in the oceans, lithogenic silicas are not important in the marine Si cycle. Biogenic silica is most concentrated within the euphotic zone of the oceans where most of it is formed. Additionally, $BSiO_2$ concentrations are highest in coastal areas, upwelling zones, and high latitude waters (often >10 μmol Si l^{-1}; Nelson et al. 1981, Nelson et al. 1987), primarily due to the elevated concentrations and supply of $Si(OH)_4$ in these areas, which allows more production of $BSiO_2$. Silicic acid concentrations ($[Si(OH)_4]$) show similar trends to $BSiO_2$ in surface waters, with elevated concentrations in coastal areas, upwelling zones, and high latitude (generally >20μM). However, $[Si(OH)_4]$ are highest in the deep sea, where concentrations often exceed 100 μM as a result of *in situ* dissolution of $BSiO_2$,. In marine surface waters, both $Si(OH)_4$ and $BSiO_2$ are least abundant in the subtropical gyres (both <1 μmol Si l^{-1}; Nelson & Brzezinski 1997). High ambient $[Si(OH)_4]$ and/or high supply rates of $Si(OH)_4$ are necessary in order to produce high $BSiO_2$ concentrations. Therefore the abundance of siliceous organisms is directly related to the availability of dissolved Si, and predominance of such species can only proceed in areas where the supply of $Si(OH)_4$ is high relative to the rates of dissolution and loss from the system.

The availability and supply of $Si(OH)_4$ in marine surface waters are controlled by a variety of biological and physical factors. Production of $BSiO_2$, via biological uptake of dissolved Si and conversion to particulate Si, is the only process in ocean waters that decreases $[Si(OH)_4]$ in a water mass. $BSiO_2$ production can increase the rate at which $Si(OH)_4$ is recycled in the surface layer, through dissolution of the newly formed and increasing pool of $BSiO_2$, but cannot supply additional $Si(OH)_4$ to the system. Therefore, there is no biological process which can supply more $Si(OH)_4$ to surface waters, yet biology is the only method for $Si(OH)_4$ removal. Furthermore, the decrease in $[Si(OH)_4]$ associated with $BSiO_2$ production and the resupply of $Si(OH)_4$ via dissolution depends on the residence time of the $BSiO_2$ in surface waters. Longer retention of biogenic particles in the surface layer would allow for more dissolution and recycling of $Si(OH)_4$, whereas

more rapid $BSiO_2$ export would decrease the time over which dissolution could occur, and would therefore remove more $Si(OH)_4$. The residence time of $BSiO_2$ in surface waters is controlled by loss rates including passive sinking (individual or aggregate cells), active downward transport within the gut of migrating organisms, sinking in fecal pellets, advection in a subducting water mass, and vertical mixing with deeper water.

Physical processes ultimately control the supply of $Si(OH)_4$ to the surface ocean. Silicic acid inputs are achieved through vertical or horizontal advection, vertical mixing, and vertical diffusion from below the surface mixed layer. As previously mentioned, $[Si(OH)_4]$ is highest in deep water masses (>100 μM). Therefore, molecular diffusion of $Si(OH)_4$ will always occur from areas of high concentration to areas of low concentration, or from deep water masses to surface water masses. Any process which mixes deeper water into the surface layer will further increase the supply of $Si(OH)_4$ to the surface layer, and consequently increase the ambient $[Si(OH)_4]$. Examples of these processes include upwelling, eddies and meanderings of currents, frontal/water mass boundaries, convective turnover, and mixing due to elevated wind stress (i.e. storms). All of these processes can increase the rate at which Si is transported upward into the surface layer from deeper water masses, and are the most important factors controlling $Si(OH)_4$ supply to surface waters in oceanic environments. Since ~85% new $Si(OH)_4$ is supplied to the marine environment via rivers (Tréguer et al. 1995), this input is confined to coastal surface waters. In coastal or nearshore regions freshwater input could be the most important factor in controlling surface $Si(OH)_4$ supply. However, river plumes are typically very localized due to their variable flows, sporadic occurrence and limited spatial extent. Furthermore, the rate of global $BSiO_2$ production is much greater than the rate of input, and therefore requires supply of surface layer $Si(OH)_4$ from deeper, high nutrient waters in order to sustain the present biological Si cycle. In general, injection of $Si(OH)_4$ via increased mixing, especially during storms and in winter, is the primary source of $Si(OH)_4$ to the surface mixed layer.

Several types of single-celled oceanic organisms produce solid silica structures, including diatoms, silicoflagellates, and radiolarians. Of these, diatoms are the only abundant primary producers that require silicon in order to grow, and are the major producers of $BSiO_2$ in the ocean (Lisitzin 1972). Diatoms have an absolute requirement

for dissolved Si, which they take up primarily in the form of $Si(OH)_4$, in order to form new frustules prior to cell division. If there is insufficient Si dissolved in seawater to form a new frustule, diatom cell division will be suspended until the Si requirement is met (Brzezinski et al. 1990), making Si a potentially limiting macronutrient for diatoms. Recent studies have revealed ambient [$Si(OH)_4$] can severely limit diatom Si-production and indicate diatom growth may be limited by Si availability in a variety of marine environments (e.g. Brzezinski & Nelson 1996, Nelson & Dortch 1996, Nelson et al. in press). It is important to note that Si uptake by diatoms can be Si-limited without diatom growth being limited because the Si-requirement of most diatoms is very flexible. For example, some diatoms can produce thinner frustules or eliminate spines under Si-limitation, while maintaining relatively high growth or division rates (Harrison et al. 1977, Brzezinski et al. 1990). Under nutrient replete conditions, diatoms typically contain ~1 mole Si for every mole N (Brzezinski 1985). All organisms require nitrogen for metabolic processes. The fact that diatoms contain nearly equal amounts of Si relative to N emphasizes the importance of Si to diatoms.

Diatoms are globally important primary producers, due to their ubiquitous and abundant distribution in most aquatic environments. As photosynthetic primary producers, diatoms require light and nutrients in order to synthesize organic compounds from inorganic CO_2, and are therefore confined to the well-lit surface layer of the ocean, commonly referred to as the euphotic zone. The fact that diatoms require Si for growth effectively links the Si and C cycles. Tréguer et al. (1995) estimated that diatoms account for ~40% of global oceanic primary production. This finding emphasizes the importance of Si in global primary production via diatoms. Diatoms have been found to be the major primary producers in coastal and high latitude environments, and also in upwelling areas (Nelson 1981, DeMaster et al. 1992, DeMaster et al. 1996). As mentioned earlier, diatoms are not predominant in mid-ocean gyres, likely due to the low supply of $Si(OH)_4$ in those environments. Because of their relatively large size and dense frustules, diatoms are the major sources of inorganic and organic sinking flux in the ocean (Michaels & Silver 1988, Buesseler 1998). Diatoms, unlike many smaller phytoplankton, have the tendency to sink out of the surface mixed layer, especially upon nutrient depletion (Alldredge & Gotschalk 1989). In coastal areas viable diatoms have

been shown to sink to the ocean bottom under bloom conditions with very low surface mixing, and consequently produce uniform chlorophyll (chl) *a* concentrations throughout the water column (Townsend et al. 1992). The export of diatom biomass out of the surface layer supplies organic carbon to the deep sea and the benthos. Diatoms also have high growth rates compared to other phytoplankton (often >1 divison d^{-1}), especially under nutrient-replete conditions, and can subsequently out-grow other phytoplankton species, resulting in diatom blooms (Banse 1982, Furnas 1990, Tang 1995). These blooms represent important events in the marine carbon cycle by episodically exporting $BSiO_2$ and organic matter formed in the surface layer and supplying it to the deep ocean and sediments (Billet et al. 1983, Lampitt 1985, Alldredge & Gotschalk 1989, Townsend et al. 1994, Buesseler et al. 1998). These bloom events can represent a large fraction of both surface primary production and supply of organic matter to the benthos in many oceanic environments (Billet et al. 1983, Parsons et al. 1984, Smetacek 1985, Smayda 1990). The high growth rates also allow diatoms to outgrow other phytoplankton, and thus to dominate primary production and export production in many nutrient replete marine environments. Therefore, due to their abundance, high growth rates, and contribution to sinking flux, diatoms are very important contributors to marine primary production and the marine carbon cycle.

Diatoms are important components in the global carbon cycle primarily because of their importance in removing organic C from the euphotic zone and supplying it, indirectly or directly, to the deep ocean. Diatoms can be lost from the surface layer through a variety of processes. Passive sinking of intact cells occurs, but sinking is much more effective when aggregates of cells, commonly called marine snow, are formed (Lampitt 1985, Alldredge & Gotschalk 1989). This method of export is particularly important in spring bloom scenarios in which diatoms outgrow their zooplankton grazers and coagulate together and sink en masse. Loss of cells via vertical mixing is also an important process, in which diatoms are mixed out of the euphotic zone through increased mixing or vertical transport in a subducting water mass (Townsend et al. 1994). This process is especially important in areas with sporadic but intense mixing events separated by periods of very low mixing. Indirect sinking of diatom biomass occurs via grazers. Typically, diatoms are not effectively grazed by small herbivores such as

microzooplankton due to their relatively large size, and are instead most likely to be consumed by larger meso- and macrozooplankton (Frost 1991, Legendre & Le Fevre 1995, Froneman & Perisinotto 1996). Typically larger zooplankton produce larger fecal pellets than their microzooplankton counterparts, and therefore these pellets have higher sinking rates (Komar et al. 1981, Fortier et al. 1994). In this way, diatom derived material can often be exported to the deep sea much more efficiently and quickly than phytoplankton consumed by micrograzers.

Given the importance of diatoms to global primary production, organic matter export, and the marine cycles of Si and C, it is advantageous to quantify their significance to each component in order to better understand the relationship between diatom production and export. The objective of this study was to quantify the surface layer Si cycle in the Pacific sector of the Southern Ocean during a series of four cruises which took place from austral spring 1997 to fall 1998. The Southern Ocean has long been recognized as a major site of high diatom biogenic silica accumulation and burial in sediments (DeMaster 1981). The abundance of diatomaceous sediments underlying the Southern Ocean could imply high diatom production, and thus high primary production in the overlying surface waters. However, previous estimates of $BSiO_2$ production in the Southern Ocean have been estimated to be close to the global mean, and primary production is 2-3 times lower than the global mean (Nelson et al. 1995, Antoine et al. 1996). These comparisons must be viewed with caution because the scarcity of $BSiO_2$ production and even primary production measurements in the open Southern Ocean has limited the certainty with which these rate measurements can be compared to the apparently high sediment accumulation of $BSiO_2$. One explanation of the apparent discrepancy between low diatom production in surface waters but high accumulation in sediments is that $BSiO_2$ is preserved in the sediments much more efficiently than in other areas of the ocean (Nelson et al. 1995). Other hypotheses include high but unmeasured $BSiO_2$ production in the surface waters (Pondaven et al. 2000), high preservation of rapidly exported $BSiO_2$, and/or opal sediments that have been focused leading to regional accumulation rates that are much too high (De Master, submitted). This study was designed to evaluate these hypotheses by measuring seasonal production, accumulation, and removal of $BSiO_2$ from the surface layer of the Southern Ocean, and to relate these

surface signals to various biological and physical factors, as well as to various $BSiO_2$ flux rates.

This study is the first attempt to measure all components of the surface layer Si cycle in the Southern Ocean over a large spatial scale, and through an entire spring to fall growing season. The Si cycle is extremely important, especially in the Southern Ocean, where the globally highest surface layer [$Si(OH)_4$] occur. Futhermore, since $Si(OH)_4$ and its dissociation products account for nearly 100% of dissolved silicon in seawater (Stumm and Morgan, 1981) and particulate silica occurs only in biogenic and lithogenic forms, the biogeochemical cycle of Si in the ocean is relatively simple, especially compared to other nutrient cycles. Therefore, interpretations of changes in any component of the Si cycle are more robust than if other unknown or unquantified forms of the element, such as dissolved organic Si, existed.

This study was part of the U.S. JGOFS sponsored Antarctic Environmental and Southern Ocean Process Study (AESOPS), designed to characterize the major biogeochemical (C, N, and Si) fluxes in the Pacific sector of the Southern Ocean. As a result, there are many other data sets of biological, chemical, and physical parameters collected simultaneously with our Si data. Some of these other data will be used to analyze observed trends in components of the Si cycle in relation to various environmental parameters.

Chapter 2:

The Si Cycle in the Pacific Sector of the Southern Ocean: Seasonal Diatom Production in the Surface Layer and Export to the Deep Sea

This chapter closely follows a submitted manuscript of the same title and authored by

Daniel E. Sigmon, David M. Nelson, Mark A. Brzezinski

In press in Deep-Sea Research II,
Elsevier Science Ltd., Oxford, UK
September 2000, submitted
June 2001, revised
July 2001, accepted

INTRODUCTION

Diatoms are the dominant phytoplankton and also the primary source of deep-sea sediments around Antarctica (DeMaster 1981). Aided in part by their relatively high sinking rates and slow dissolution, sinking diatom frustules accumulate on the seafloor, forming biogenic silica sediments, or siliceous ooze. Southern Ocean sediments account for >30% of all biogenic silica burial worldwide (Tréguer et al. 1995, DeMaster submitted). Light conditions are not favorable for phytoplankton growth most of the year in the Southern Ocean due to short daylight hours, deep wind mixing, and ice cover. However, when conditions do become favorable for growth, diatoms are able to exploit nutrient-replete conditions and can quickly consume dissolved Si, converting it to $BSiO_2$ (Brzezinski et al. in press), which then supports the rapid export of Si from the surface layer to the deep ocean (Honjo et al. 2000). This process also exports diatom carbon from the surface layer to the deep ocean, making diatom blooms important in both the Si and C cycles of the Southern Ocean. However, the export of Si and C from the surface layer appear to be decoupled in the Southern Ocean compared to most other marine environments. The Southern Ocean accounts for a large fraction of the global Si burial but <4% of the marine primary production and organic C burial (Nelson et al. 1995). Therefore, the Southern Ocean may presently be a system with high production and export of $BSiO_2$, but low production and export of organic matter.

The Southern Ocean includes both Antarctic and sub-Antarctic waters, where circulation is dominated by the eastward flowing Antarctic Circumpolar Current (ACC). The ACC is characterized by a series of embedded circumpolar physical and chemical fronts which separate it from waters to the north, as well as delimiting different waters within the Southern Ocean (Belkin & Gordon 1996). Sub-Antarctic waters are constrained by the Subtropical Front (STF) to the north and the Antarctic Polar Front (APF) to the south. Antarctic waters are found only south of the APF (Gordon 1967). The Southern ACC Front (SACCF) is another front embedded within the ACC, and separates coastal, Ross Sea Gyre, and Weddell Sea Gyre water from the ACC. The STF typically corresponds to a nitrate gradient, with values increasing to around 20 μM south of the front, and depleted to <5μM in the warmer sub-tropical waters to the north

(Lutjeharms et al. 1985, van Bennekom et al. 1988). The APF corresponds to a very strong [$Si(OH)_4$] gradient in austral winter, with concentrations increasing to the south. It is not uncommon to observe an increase in [$Si(OH)_4$] of 20-30 μM across 1° latitude at the APF in spring (Lutjeharms et al. 1985, van Bennekom et al. 1988, Brzezinski et al. in press). The poor light conditions in Southern Ocean winter effectively prevent significant diatom growth, therefore allowing upwelled nutrients to accumulate in surface waters. In the Pacific sector sea ice can extend as far north as the southern edge of the APF (Moore et al. 1999). As the season progresses toward spring, light increases and the ice begins to retreat southward. By summer, the location of the [$Si(OH)_4$] gradient can become uncoupled from the physical location of the APF, and begins to shift southward in response to diatom growth and $Si(OH)_4$ uptake (Le Jehan & Tréguer 1983, Brzezinski et al. in press). The resupply of $Si(OH)_4$ via increased mixing during winter replenishes the surface layer, restoring the gradient to the location of the APF. Resupply of nutrients is, however, a continual process since the ACC is a generalized area of upwelling (e.g. Comiso et al., 1993). It is not until biological uptake of the nutrients declines in fall that net resupply to the surface layer occurs.

The objective of this paper is to estimate seasonal $Si(OH)_4$ removal and $BSiO_2$ accumulation and export from the surface layer of the Southern Ocean along 170° W, based on a Si budget for the upper 50 m. This budget is constructed by calculating depth-integrated drawdown of $Si(OH)_4$ and accumulation of $BSiO_2$ over the growing season. These two components of the Si cycle are combined to provide an estimate of total surface layer Si, and its export from the surface layer based on changes in pool sizes between November 1997 and March 1998. The integrated export provides a minimum estimate of net seasonal Si export from the surface layer, and can be compared to other estimates of $Si(OH)_4$ removal and $BSiO_2$ export, including gross and net $BSiO_2$ production rates, sediment trap collection rates, ^{234}Th-based export estimates, and seabed flux and accumulation rates.

METHODS

The data presented in this paper were collected on a series of four cruises beginning on 26 October 1997 and ending on 15 March 1998. The cruises took place in austral spring and summer, and each were ~5 weeks long, with sample collection occurring for ~4 of those weeks. Sampling was performed primarily in November on the first cruise; entirely during December on the second cruise; entirely during January on the third cruise; and from mid-February to mid-March on the fourth. Cruise tracks followed along 170° W and the latitudinal range of the cruises spanned from 53° to 71.5° S, depending on the location and extent of sea-ice, as well as the type of cruise. This paper will focus on the area from 58° to 68° S.

Eight depths were sampled at each station, and corresponded to 85, 50, 25, 18, 10, 5, 1, and 0.1% of sea-surface irradiance. Data on sampling depth, $[Si(OH)_4]$ and $BSiO_2$ concentrations from all profile stations are provided in the Appendix. Samples were taken from the same sampling bottle for $Si(OH)_4$ and $BSiO_2$ concentrations, Si uptake rates, and silica dissolution rates. All of these measurements were made at every depth on all profile stations where light depth was known. $Si(OH)_4$ concentrations were determined with a modification of the Strickland & Parsons (1972) standard colorimetric method (Brzezinski & Nelson, 1989). $BSiO_2$ concentrations were determined after NaOH digestion, follwed by HF digestion for $LSiO_2$ concentrations (Brzezinski & Nelson 1989). Determination of Si production rates are described in Brzezinski et al. (1997). $BSiO_2$ dissolution rates were determined using the isotope dilution method described in Nelson & Goering (1977). Detailed methodology of sample collection, parameters measured, and experiments performed are detailed in Brzezinski et al. (in press) and Nelson et al. (in press). Mixed layer depth was also determined for each station profile. The criteria used here is the depth at which the potential density anomaly differed from the surface value by 0.01 kg m^{-3}, and is a measure of the depth of active mixing (Brainerd & Gregg 1995).

Station profile data and some surface data for $[Si(OH)_4]$ and $BSiO_2$ were objectively contoured using Surfer 6.0. All contouring was constrained to the latitudinal range between 56° S and the southernmost station sampled for each cruise. All grid files

used for contouring had identical horizontal and vertical resolution. Therefore, the grid files for each cruise had the same number and distribution of grid points per meter of depth or degree latitude. The contours were visually inspected against measured concentrations to assure accurate representation of the data.

Depth-integrated concentrations were calculated for $Si(OH)_4$ and $BSiO_2$ at every station between 58° and 68°S for all four cruises. Values for the $BSiO_2$ pool were integrated to the base of the euphotic zone, defined here as the depth where light was reduced to 0.1% of surface irradiance. Values for the $Si(OH)_4$ pool were integrated between the surface and 50 m, because that was the deepest depth sampled at some stations. The only valid way to compare temporally offset, but spatially similar estimates of integrated $Si(OH)_4$ is to integrate to a fixed and uniform depth for all stations and all times, and that uniform depth was limited by the shallowest euphotic zone (~50 m). However, the $BSiO_2$ pool estimates were extended to the base of the euphotic zone at each station in order to include biomass that was produced in the upper 50 m and sank to greater depths. The assumption that no significant biogenic silica was produced below 50 m is supported by very low ^{32}Si uptake rates in water samples collected below 50 m (values below 50 m were always <0.075 μmol Si l^{-1} d^{-1}, compared to values within the bloom of >1.5 μmol Si l^{-1} d^{-1}, Brzezinski et al. in press). Integrated $BSiO_2$ concentrations for each station sampled are given in Brzezinski et al. (in press). The integrations were performed by trapezoidal integration between the surface and either the base of the euphotic zone or 50 m. Integrated concentrations for each Si pool were binned into 1° latitude bands centered at each whole degree. On the rare occasions when no stations were occupied inside a degree band during a given cruise, integrated values for each pool were interpolated by averaging the two closest stations (the closest one on either side of the latitude in question).

Initial concentrations of $BSiO_2$ at all degree bands under ice (64° to 68° S in November, and 66° to 68° S in December) were assumed to be 25 mmol Si m^{-2}, which corresponds to 0.5 μmol Si l^{-1} throughout the upper 50 m. This represents an average value for spring under-ice concentrations in the Weddell Sea (Nelson et al. 1987), and is probably an upper estimate for under-ice $BSiO_2$ in the open ocean. Under-ice $[Si(OH)_4]$ were assumed to be 60-70 μM, or 3,000-3,500 mmol m^{-2}. These values are typical of

winter surface layer concentrations in the ACC between 63° and 66° S, according to concentrations measured in the temperature minimum layer (data available at www.usjgofs.whoi.edu). The temperature minimum layer located between 63° and 66° S was –1.7° C, and was therefore not significantly altered from the freezing temperature at which this water was formed. A similar approach using nutrient concentrations in the temperature minimum layer (winter remnant water) has been used in the Weddell Sea (Jennings et al. 1984).

Decreases in the $Si(OH)_4$ pool on each successive cruise in each degree band were used to estimate net $Si(OH)_4$ removal (Table 1). Increases in the $BSiO_2$ pool were used to estimate net $BSiO_2$ accumulation in the surface layer over the growing season (Table 2). Changes in pool sizes were determined by subtracting the integrated Si pool size for a given month from the integrated pool size from the subsequent month, within the same latitude degree band. Therefore, negative changes indicate net loss, whereas positive changes indicate net gain in Si (Table 1-3). Positive changes in the dissolved pool (resupply of $Si(OH)_4$, which occurred only between January and March) were not used to estimate seasonal drawdown of $Si(OH)_4$ or export of Si. The two Si pools ($Si(OH)_4$ and $BSiO_2$) were then summed to obtain estimates of total Si present in the upper 50 m for each degree band during each cruise. Decreases in total surface layer Si with each degree band were then used to calculate total Si export from the upper 50 m. Total seasonal $Si(OH)_4$ removal, $BSiO_2$ accumulation, and total Si export are simply the sum of those changes between each cruise for each pool, relative to the initial concentrations in November. The growing season is defined as the period during which diatoms were actively growing (net production of $BSiO_2$), and excludes periods before or after the cruises, when no data on $BSiO_2$ production were obtained.

The 50 m total Si export estimates were used to compare net changes in total surface layer Si with $BSiO_2$ fluxes collected by sediment traps at 1000 m (Honjo et al. 2000). Therefore, the surface layer Si export estimate for each degree band was placed in latitudinal bins which most closely corresponded to the location of sediment traps located at 56.9°, 60.2°, 63.2°, and 66.1° S (Honjo et al. 2000). The latitudinal bins used to compare to the moored sediment traps were 55-58° S (north of the APF), 59-61° S (the APF), 62-65° S (the seasonal ice zone of the ACC), and 66-68° S (south of the SACCF).

Therefore the assigned latitudinal bins corresponded to distinct hydrographic zones (based on temperature, salinity, and nutrient concentrations), each of which contained one sediment trap mooring. The calculated changes in Si export for all latitudes within each bin were averaged to estimate the integrated flux of Si out of the surface layer for that latitude range (e.g. the change between 62° and 65° S is an average of the 4 latitude bands within the bin).

RESULTS

Station Profiles

Contours of $[Si(OH)_4]$ collected during station profiles for all cruises, along with station locations and sample depths, are shown in Fig. 1. During the first cruise in November 1997, corresponding to austral spring, there was a pronounced meridional $[Si(OH)_4]$ gradient centered between 60° and 61° S. This $Si(OH)_4$ gradient (Si front) corresponded with the location of the APF. The southern edge of the APF, which remained relatively constant throughout the sampling period, was located between 61 and 61.5° S (Moore et al. 1999). There were no observed vertical gradients in $[Si(OH)_4]$ within the upper 100 m in spring. By early summer there was clear evidence for $Si(OH)_4$ removal. By December the Si front had shifted southward, to between 62.3° and 63° S, and the gradient was stronger and more compressed. Vertical gradients in $[Si(OH)_4]$ also became established between 61° and 63° S, with concentrations increasing by ~10 μM between 40 and 50 m. During the third cruise in mid summer (January 1998), severe $Si(OH)_4$ depletion was evident, with surface concentrations <2 μM occurring as far south as 64.5° S. Consequently, the Si front was displaced further south, to 65° S, and was most compressed during this time period. Vertical gradients in $[Si(OH)_4]$ were also most pronounced during mid summer, with the steepest gradients around 65° S exceeding 30 μM between 30 and 40 m. The Si front was still located near 65° S during the Feb/March cruise, but $[Si(OH)_4]$ had increased in the upper 80 m everywhere north of 65° S. Silicic

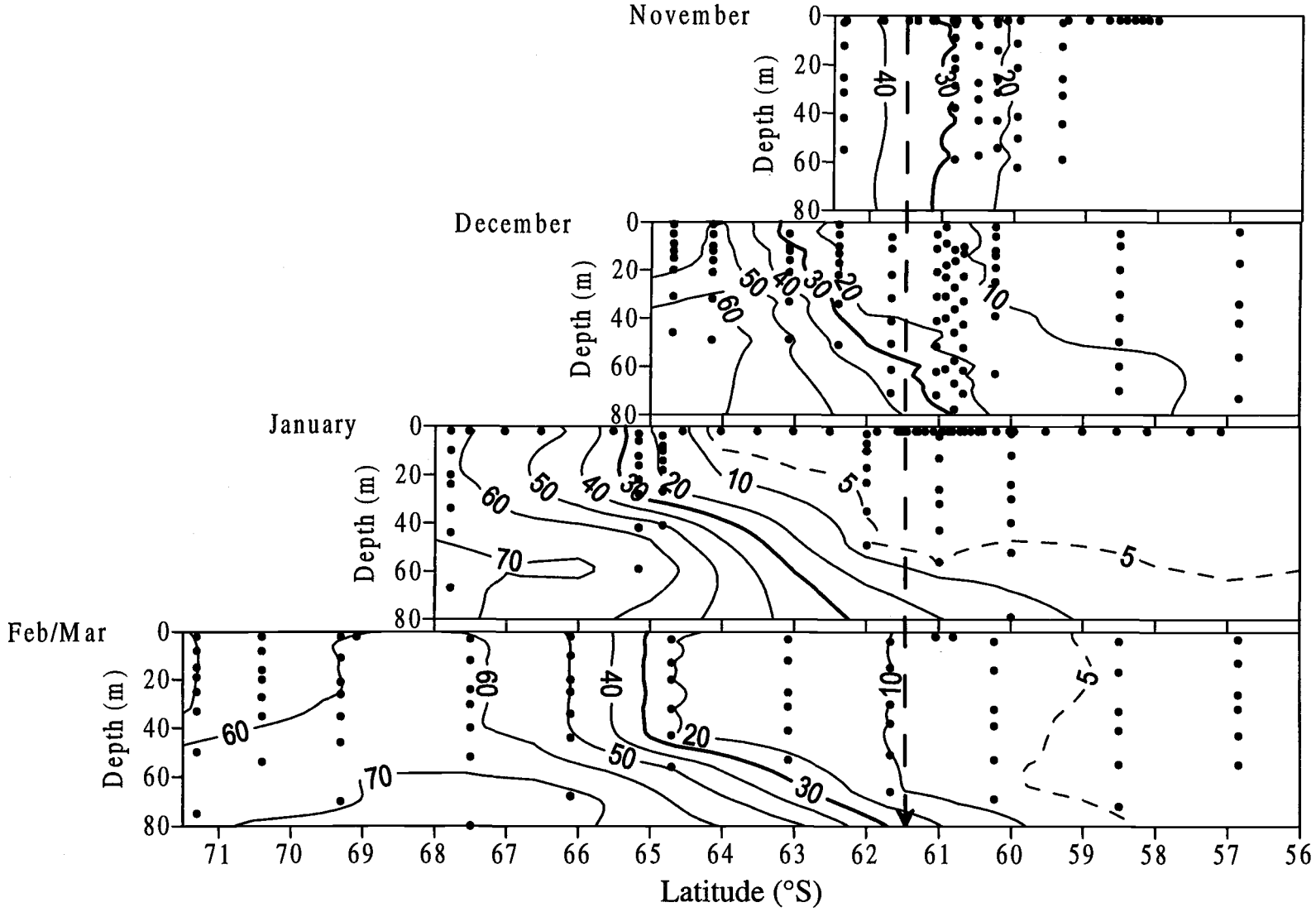

Fig. 1: Contours of $Si(OH)_4$ concentrations along 170° W with station profiles shown (dashed line represents southern edge of APF)

acid concentrations south of 66° S remained relatively unchanged between January and March. Vertical [$Si(OH)_4$] gradients were still strong in late summer between 64° and 66° S, with concentrations increasing by >30 μM between 40 and 60 m (Fig 1).

Contours of $BSiO_2$ concentrations collected during station profiles for all cruises, along with station locations and sample depths, are shown in Fig. 2. There was very little diatom biomass during the spring (November) cruise, with $BSiO_2$ concentrations <1.5 μmol l^{-1} and <125 mmol m^{-2} throughout the study area. There were no vertical gradients of $BSiO_2$ within the upper 100 m in the study area, similar to the [$Si(OH)_4$] profiles. By December $BSiO_2$ concentrations had increased significantly in the upper 80 m throughout the study area, with the highest concentrations located in the upper 40 m at 62° S. The $BSiO_2$ maximum was closely associated with the Si front. By the mid summer cruise in January, the $BSiO_2$ maximum had shifted much farther south and was centered around 65° S. The $BSiO_2$ maximum was still located within the Si front, which had also shifted southward. The magnitude and spatial extent of the diatom bloom were greatest during this time. Maximal $BSiO_2$ concentrations around 65° S exceeded 17 μmol l^{-1}, and represent the highest open ocean concentrations ever measured. There was substantial $BSiO_2$ present from the surface to 40-50 m in the core of the bloom, slightly deeper than the observed $Si(OH)_4$ depletion, indicative of sinking diatoms. By the end of summer, the only area of high $BSiO_2$ was in Ross Sea Gyre water centered on 71° S, and the magnitude of the maximum was much less than concentrations observed further to the north in December or January. It is unlikely that the high diatom biomass at 71° S is related to the diatom bloom observed within the ACC, due to the absence of elevated biomass or significant nutrient drawdown between 65° and 71° S. The decrease in $BSiO_2$ everywhere north of 68° S between January and March indicates that a large export of diatom biomass had occurred during that time (Fig 2).

Lithogenic silica ($LSiO_2$) was measured for all profile stations, but has not been reported elsewhere. $LSiO_2$ concentrations were very low throughout the study area on all cruises. Average $LSiO_2$ concentrations for the November, December, and March cruises were 0.077, 0.085, and 0.063 μmol Si l^{-1}, respectively. The range of $LSiO_2$

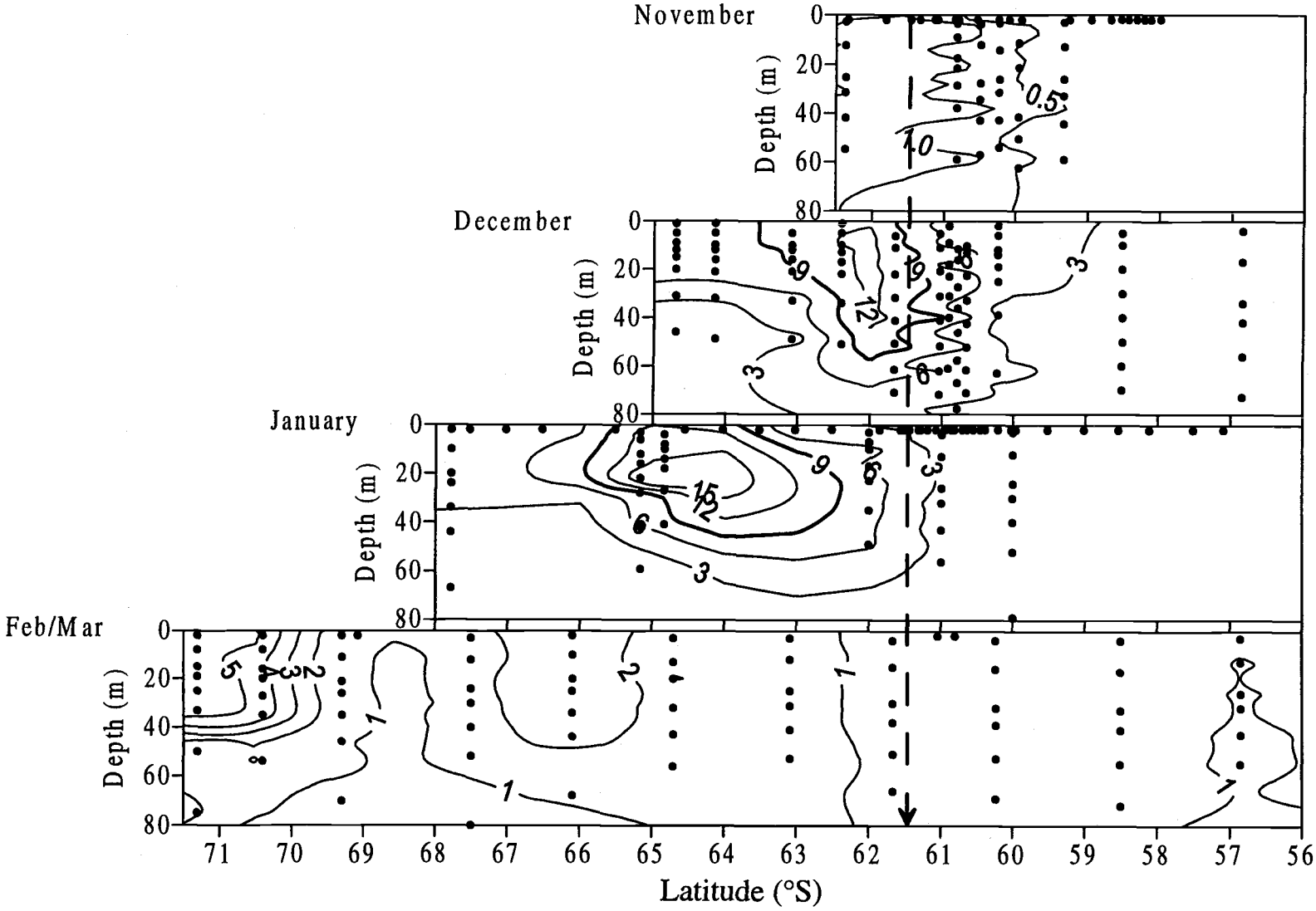

Fig. 2: Contours of $BSiO_2$ concentrations along 170° W with station profiles shown (dashed line represents southern edge of APF)

concentrations during these three cruises was 0.01 to 0.55 μmol Si l^{-1}. The average $LSiO_2$ concentrations represented 12%, 2%, and 4% of the average $BSiO_2$ concentrations in November, December, and March, respectively. Therefore, the lithogenic phase was always small compared to the biogenic phase, and comprised <4% of total particulate Si except in early spring, before significant diatom biomass had accumulated.

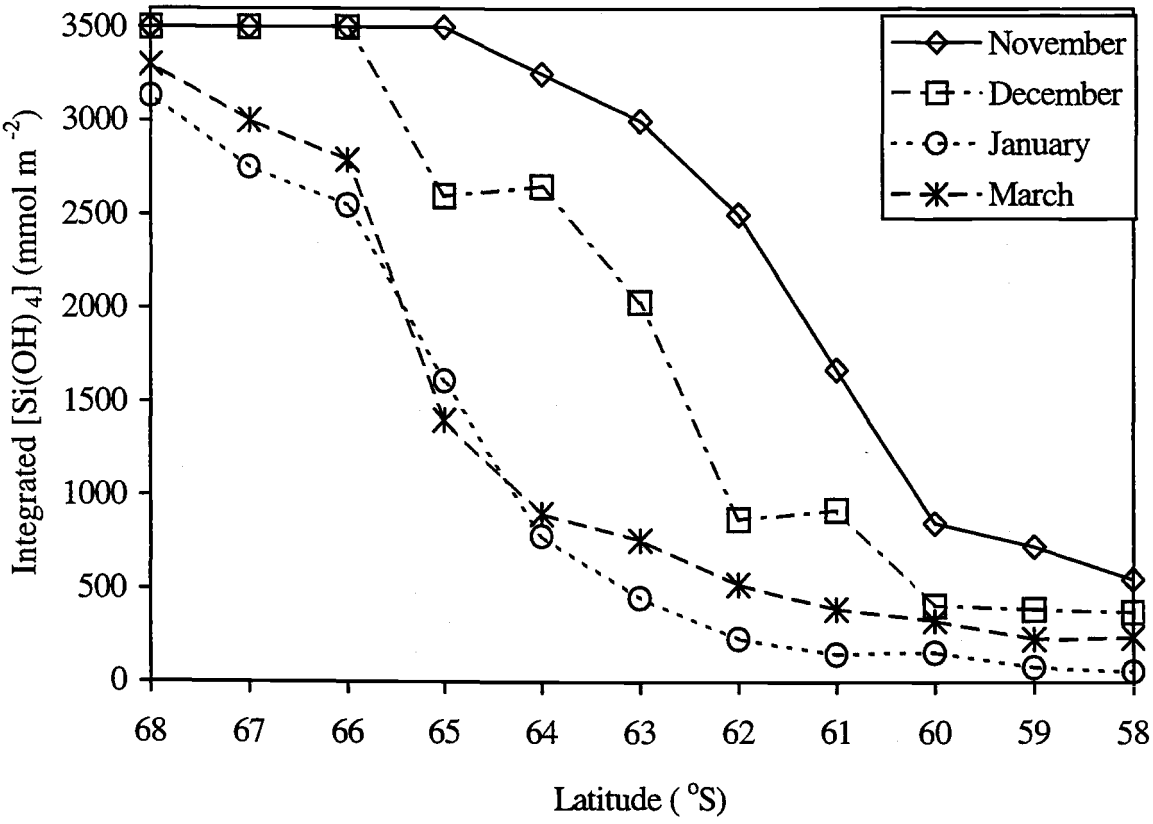

Fig. 3: Integrated $Si(OH)_4$ concentrations along 170° W between 58° and 68° S

Integrated Si Pools

Integrated concentrations of $Si(OH)_4$ also reveal the strong meridional Si gradient, which was initially centered on 61° S, associated with the APF (Fig. 3). By the end of summer (March), the Si front had been displaced 4° south and was centered on 65° S. The Si front, based on integrated concentrations, was steepest in December, with vertically integrated $[Si(OH)_4]$ increasing from 870 to 2,033 mmol Si m^{-2} between 62°

and 63° S. Interestingly, the differences in vertically integrated $Si(OH)_4$ across the 2° of latitude that included the Si front were very similar in November and January (1,650 and 1,770 mmol Si m^{-2} between 60-62° S and 64-66° S, respectively). This finding differs from the observation that the strongest gradient in surface layer [$Si(OH)_4$] based on contouring of station profiles was in January (Fig. 1). This difference can be explained by the shallow depth (~30 m) of the nutricline in January. Thus, vertical integration of [$Si(OH)_4$] included water well below the nutricline (>50 μM $Si(OH)_4$) in January, but not in December. Therefore, the steepest meridional Si gradient in the upper 30 m occurred in January, but when integrated down to 50 m, the steepest meridional gradient occurred in December.

The largest seasonal decreases in $Si(OH)_4$ (1,522-2,550 mmol m^{-2}) occurred between 61° and 65° S, with an average removal of 2,140 mmol Si m^{-2} between November and January (Table 1). This magnitude of removal translates to a net [$Si(OH)_4$] drawdown of 43 μM between November and January, at an average rate of ~27 mmol Si m^{-2} d^{-1} or 0.54 μM d^{-1}. Based on integrated concentrations, maximal net $Si(OH)_4$ removal rates of ~1 μM d^{-1} were observed in the 64° S latitude band between December and January (removal of 1870 mmol Si m^{-2} in the upper 50 m in 35-40 days).

The most striking feature apparent in this analysis is that an average of 82% (range of 54-91%) of the $Si(OH)_4$ present in the upper 50 m during November was removed by the end of January, ~80 days later, from 58° to 65° S (Table 1). Even though substantial drawdown occurred between 66° and 68° S by January, and the magnitude of that drawdown (370-950 mmol Si m^{-2}) was comparable to that between 58° and 60° S, this removal accounted for only 11-27% of the initial $Si(OH)_4$ available between 66° and 68° S at the end of winter. Therefore, the amount of $Si(OH)_4$ removed from the surface layer depends mainly on the initial $Si(OH)_4$ pool size north of, but not south of 65° S. Thus, the initial $Si(OH)_4$ pool present in surface waters at the start of the growing season appears to set an upper limit on the magnitude of potential drawdown between 58° and 65° S, assuming no inputs of $Si(OH)_4$ during summer. South of 66° S the length of the growing season, as controlled by latitude and sea ice cover, likely sets the upper limit on the amount and fraction of initial $Si(OH)_4$ that can be removed, and keeps that fraction

Table 1: Integrated silicic acid concentrations and changes (all in mmol m^{-2})

	Concentration				Net Changes			Seasonal Removal	
Latitude (°S)	Nov	Dec	Jan	Mar	Dec-Nov	Jan-Dec	Mar-Jan	Amount	% of initial
58	550	375	56	240	-175	-319	184	494	90
59	725	390	80	230	-335	-310	150	645	89
60	850	410	158	330	-440	-252	172	692	81
61	1670	920	148	390	-750	-772	242	1522	91
62	2500	870	230	520	-1630	-640	290	2270	91
63	3000	2033	450	760	-967	-1583	310	2550	85
64	3250	2650	780	900	-600	-1870	120	2470	76
65	3500	2600	1610	1400	-900	-990	-210	2100	60
66	3500	3500	2550	2790	0	-950	240	950	27
67	3500	3500	2750	3000	0	-750	250	750	21
68	3500	3500	3130	3300	0	-370	170	370	11

consistently <30%. The highest percentage removal (91%) of initial $Si(OH)_4$ occurred at 61° and 62° S, and that removal decreased consistently to the south, with the lowest percentage removal (11%) at 68° S. There was a fundamental change in biological activity seen by the February/March cruise. Vertically integrated [$Si(OH)_4$] decreased throughout the area from November through January, but by March it had increased by 120-310 mmol m^{-2} at all but one latitude band, which was located at 65° S (Table 1). The increases observed during the March cruise correspond to surface layer $Si(OH)_4$ increases of 2.4-6.2 μM relative to January. A detailed summary of the concentrations and changes in integrated [$Si(OH)_4$] between 58° and 68° S is given in Table 1.

Integrated $BSiO_2$ concentrations were highest within, or just north of the Si front during December and January. The highest concentrations of $BSiO_2$ occurred between 61° and 65° S, where integrated values exceeded 475 mmol Si m^{-2} in December or January (Fig 4, Table 2). This latitudinal range therefore comprised the main bloom region, with much lower diatom biomass measured to the north and south. The highest integrated $BSiO_2$ concentration of 700 mmol m^{-2} occurred during December, in the 62° S latitude bin. This is the highest integrated concentration of $BSiO_2$ ever measured in the open ocean. Although higher $BSiO_2$ concentrations by volume were measured in January, the deeper euphotic zones in December translated into higher integrated biomass. The largest spatial extent and magnitude of $BSiO_2$ accumulation in the euphotic zone occurred between November and December, with an average net accumulation of 330 (range of 220-575) mmol Si m^{-2} (Table 2). Assuming ~40 days between samplings within a given latitude bin results in an average $BSiO_2$ accumulation rate of 8.25 mmol m^{-2} d^{-1} between 61 and 65° S, which represents 30% of the observed drawdown of $Si(OH)_4$ in the same region. By January, $BSiO_2$ increases were less, averaging 237 mmol m^{-2}, and only increased south of 62° S, with losses from the surface layer between 58° and 62° S. The maximal $BSiO_2$ accumulation rate of 0.3 μmol Si l^{-1} d^{-1} was observed at 62° S between November and December (575 mmol Si m^{-2} in ~50 m over 40 days). The largest export of $BSiO_2$ from the euphotic zone occurred between January and March, with decreases observed everywhere between 58° and 68° S (Table 2). Maximal seasonal export of $BSiO_2$, averaging 450 mmol m^{-2}, was observed between 61° and 65° S, the

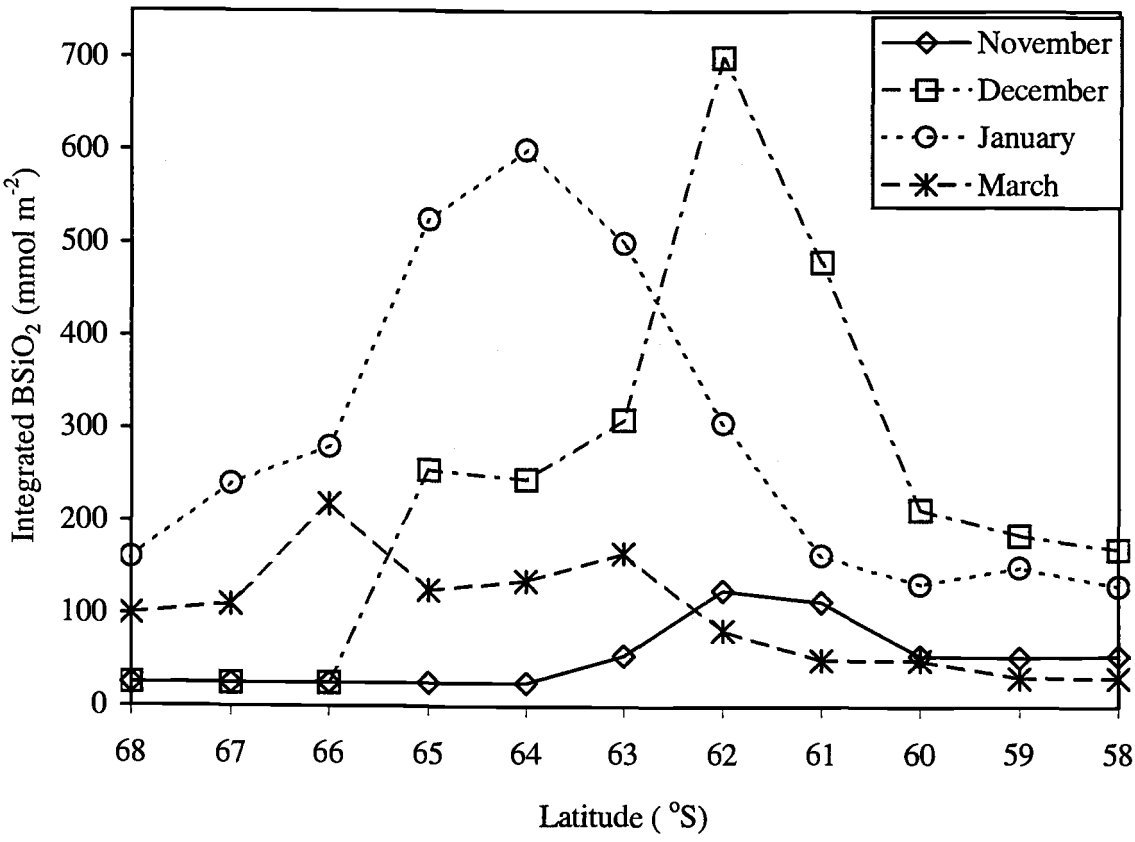

Fig. 4: Integrated $BSiO_2$ concentrations along 170° W from 58° to 68° S

Table 2: Integrated biogenic silica concentrations and changes (all in mmol m^{-2})

	Concentration				Net Changes		
Latitude (°S)	Nov	Dec	Jan	Mar	Dec-Nov	Jan-Dec	Mar-Jan
58	55	170	130	31	115	-40	-99
59	53	185	150	31	132	-35	-119
60	55	213	132	50	158	-81	-82
61	113	480	163	50	367	-317	-113
62	125	700	306	82	575	-394	-224
63	55	310	500	165	255	190	-335
64	25	245	600	135	220	355	-465
65	25	255	525	125	230	270	-400
66	25	25	280	218	0	255	-62
67	25	25	240	110	0	215	-130
68	25	25	160	100	0	135	-60

same zone where the maximal $Si(OH)_4$ drawdown was observed. Biogenic silica was certainly being produced and exported from the surface layer throughout the growing season, and therefore these estimates of export based on net changes are minimal estimates. A detailed summary of $BSiO_2$ concentrations and changes is found in Table 2.

Since conversion of $Si(OH)_4$ to $BSiO_2$ is the only removal term for $Si(OH)_4$, net $Si(OH)_4$ removal over time can be used to estimate $BSiO_2$ production during that same time period. Furthermore, since $BSiO_2$ is exported from the surface layer, the relationship between net $Si(OH)_4$ removal and $BSiO_2$ accumulation can be used to estimate the export efficiency of $BSiO_2$. Thus, the ratio of $BSiO_2$ accumulation to $Si(OH)_4$ removal over the same time period is a measure of the amount of removal that is still present in the surface layer as $BSiO_2$. The relationship between $BSiO_2$ accumulation and $Si(OH)_4$ removal within each latitude bin between 58° and 68° S was tested by linear regression analysis (Fig. 5). The data presented in Fig. 5 are totals for each 1° latitude band between successive cruises,

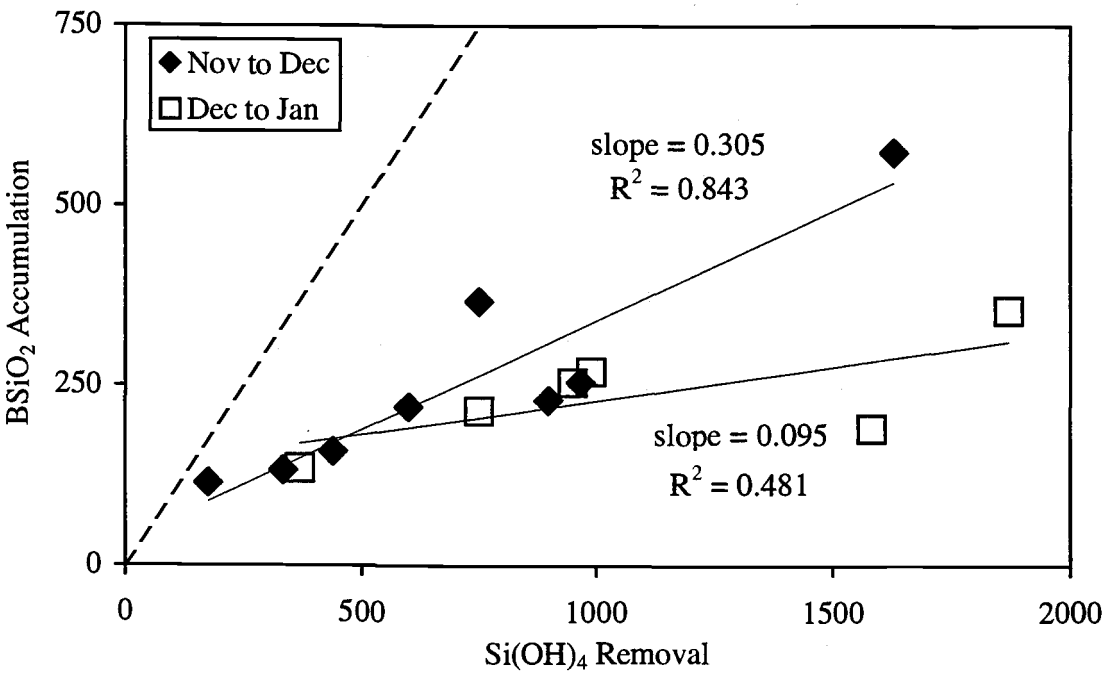

Fig. 5: Regression of integrated $BSiO_2$ accumulation to $Si(OH)_4$ removal between successive cruises during which $BSiO_2$ increased and $[Si(OH)_4]$ decreased from 58° to 68° S. The dashed line indicates a 1:1 relationship between $BSiO_2$ accumulation and $Si(OH)_4$ removal.

and therefore illustrate differences between $Si(OH)_4$ removal and $BSiO_2$ accumulation within the growing season. Net $BSiO_2$ accumulation and $Si(OH)_4$ removal between November and December occurred throughout the study area from 58° to 68° S. However, net accumulation and removal between December and January occurred only between 63° and 68° S. No $BSiO_2$ accumulation occurred between January and March from 58° to 68° S. This analysis reveals a positive linear relationship between $Si(OH)_4$ removal and $BSiO_2$ accumulation between November and December, with an R^2 value of 0.843 and a slope of 0.3 (s.d. = 0.05, $p < 0.001$). There is no significant relationship between removal and accumulation between January and March, with an R^2 value of 0.48 and a slope of 0.1 (s.d. = 0.05, $p = 0.126$), indicating that the slope of the line is indistinguishable from zero. The slopes of the two regression lines were significantly different from each other at the 95% level ($Z = 1.72$, $p = 0.043$).

A 1:1 relationship (slope = 1) between these two variables would mean that all of the observed removal of $Si(OH)_4$ was measured as $BSiO_2$ accumulation. However, the relationship between removal and accumulation between November and December indicates that 30% ± 10% (slope = 0.3) of the $Si(OH)_4$ removed from the upper 50 m during that time period was still present as accumulated $BSiO_2$ in December. Between December and January, only 10% ± 10% of the observed removal during that time period was still present as $BSiO_2$. The difference between the solid regression lines and the dashed 1:1 line is a measure of $BSiO_2$ export. Therefore, this analysis indicates that the other 70% and 90% of $Si(OH)_4$ removed from November to December and from December to January, respectively, had been exported as $BSiO_2$ during that same time period. This analysis also indicates that the retention of diatom biomass in this system decreases during the growing season, with increased export in late summer compared to early summer.

Total Si is equal to the sum of the dissolved and particulate Si pools. Net Si export estimates are the changes in total surface layer Si over time. Both total Si pool size and Si export are presented for each cruise and as the differences between subsequent cruises (Table 3). Since export is a loss term, decreases in both pools lead to larger export estimates than if one pool decreased while the other increased or remained unchanged. This method uses the initial conditions measured in November to estimate

Table 3: Total surface layer Si concentrations and changes (all in mmol m^{-2})

	Total Si present				Net Changes in Total Si			Seasonal Si Export	
Latitude (°S)	Nov	Dec	Jan	Mar	Dec-Nov	Jan-Dec	Mar-Jan	Amount	% of initial
58	605	566	186	271	-39	-380	85	419	69
59	778	575	230	261	-203	-345	31	548	70
60	905	623	290	380	-282	-333	90	615	68
61	1783	1400	311	440	-383	-1089	129	1472	83
62	2625	1570	536	602	-1055	-1034	66	2089	80
63	3055	2343	950	925	-712	-1393	-25	2130	70
64	3275	2895	1380	1035	-380	-1515	-345	2240	68
65	3525	2855	2135	1525	-670	-720	-610	2000	57
66	3525	3525	2830	3008	0	-695	178	720	20
67	3525	3525	2990	3110	0	-535	120	560	16
68	3525	3525	3290	3400	0	-235	110	260	7

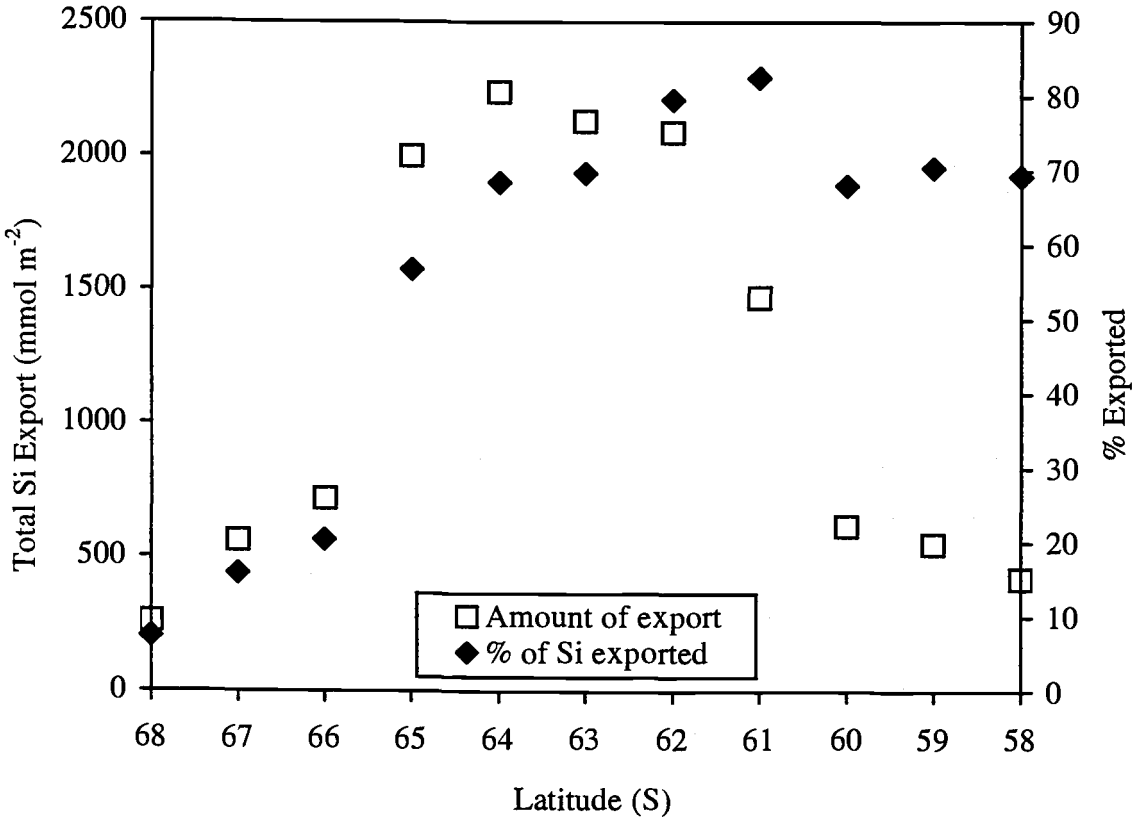

Fig. 6: Total integrated Si export from the upper 50 m and the % of initial Si this export represents

the initial total Si pool size at the beginning of the growing season. Since the dissolved pool accounted for the majority of total Si throughout the study period, export estimates closely matched changes in integrated $[Si(OH)_4]$, with an average export of ~2,000 mmol Si m^{-2} by late January between 61° and 65° S (Fig. 6, Table 3). More than 57% of that seasonal export, or 1,150 mmol m^{-2}, occurred between early December and late January. The region of highest Si export from the surface layer matches the bloom region as expected. The seasonal total Si export from November to March accounted for an average of 71% (range of 57-83%) of the initial total Si in the surface layer between 58° and 65° S, but only 15% between 66 and 68° S (Fig. 6). A detailed summary of total Si and Si export is given in Table 3.

Physical vs. Biological Control

Euphotic zone depth

Most of the station profiles throughout the study period had sample depths confined to the euphotic zone (described in methods section). For this study, the euphotic zone is defined as the depth interval between the surface and the 0.1% light depth (the depth to which 0.1% of surface-incident light reaches). Mixed layer depths were also determined at each station. Therefore, relationships of measured biological parameters to euphotic zone depth and mixed layer depth could be analyzed. Analyses involving euphotic zone depth (EZD) allows measured parameters to be compared between different stations at the same light depth, regardless of the actual sample depth. However, the depth of active mixing is very important in vertical structure of phytoplankton biomass and growth, as well as nutrient concentrations and gradients, and will also be discussed.

All stations where euphotic zone depth was measured were used to compare depth-averaged water column $BSiO_2$ and chl *a* to EZD. Since no *a priori* relationships between the parameters were chosen, regression analyses were performed to obtain the best-fit empirical relationships between EZD and $BSiO_2$ or chl *a*. A strong negative relationship between $BSiO_2$ concentration and EZD was discovered (Fig. 7). Increasing $BSiO_2$ concentrations were indicative of shallower euphotic zone depths. In fact, all stations with >3 μmol Si l^{-1} had EZD <90 m, while all stations with average $BSiO_2$ <3 μmol l^{-1} had EZD >100 m. Regression analysis (SPSS) of the effect of average $BSiO_2$ concentrations on EZD revealed that the negative relationship was best described by a logarithmic function, with an adjusted-R^2 = 0.835 and a p-value <0.0001 (Fig. 7). Given that suspended particles control the penetration of light through the water column via absorption and scattering, an interpretation of this result is that $BSiO_2$ concentration was a significant controller of light penetration, and thus of EZD.

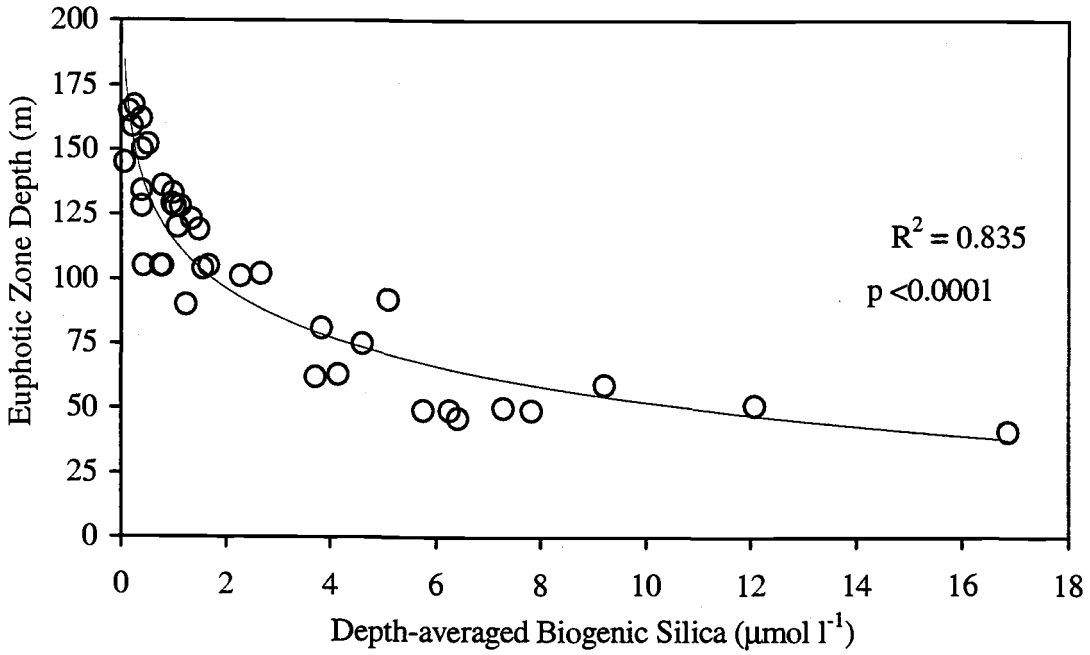

Fig. 7: Regression of euphotic zone depth as a function of average $BSiO_2$ concentration for all profile stations

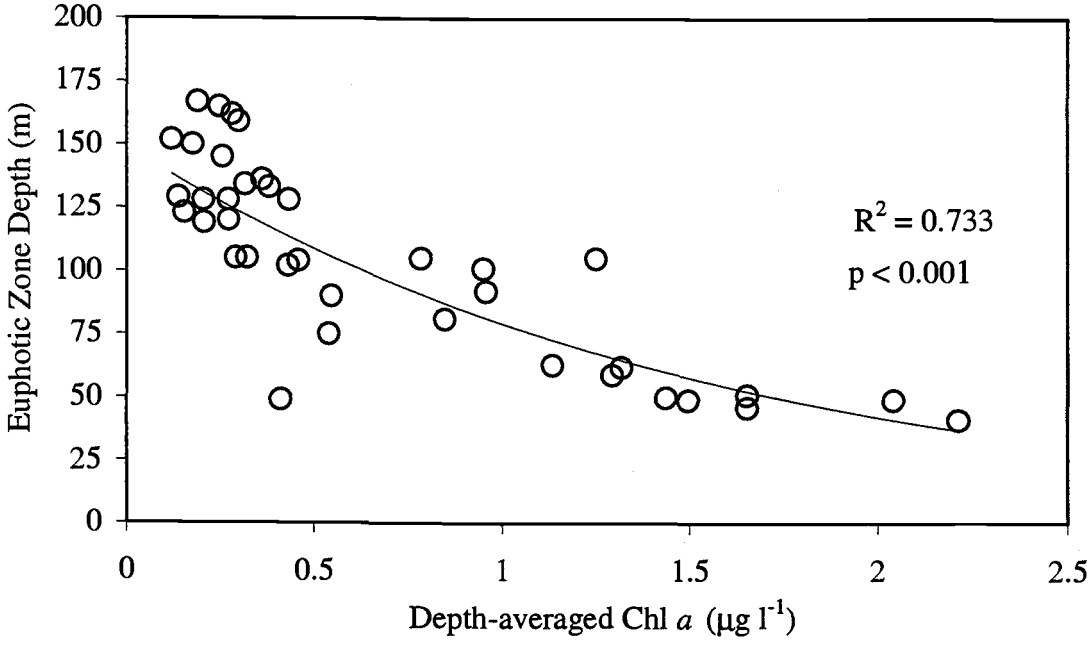

Fig. 8: Regression of euphotic zone depth as a function of average chl *a* concentration for all profile stations

Flurometric chl *a* data were also collected at all depths and stations where $BSiO_2$ was measured (supplied by W.O. Smith, and available at http://usjgofs.whoi.edu). These data were also used in regression analysis with EZD. The analysis revealed a strong negative relationship and produced an exponential best-fit line with an adjusted-$R^2 = 0.733$ and a p-value <0.001 (Fig. 8). On a seasonal basis, $BSiO_2$ concentration was a slightly better predictor of EZD than average chl *a* concentration, but both parameters likely exerted considerable control on the euphotic zone depth via light absorption.

A correlation analysis comparing all data of average euphotic zone $BSiO_2$, an indicator of diatom biomass, and chl *a*, an indicator of total phytoplankton biomass, was also performed. One would assume these two biomass parameters would co-vary if diatoms are the main primary producers south of the APF. A positive relationship was discovered between the 2 parameters, with a Pearson's r = 0.823 and a p-value <0.001 (Fig. 9). Increasing $BSiO_2$ concentrations were significantly correlated with increasing chl *a* concentrations. However, there is considerable scatter in the

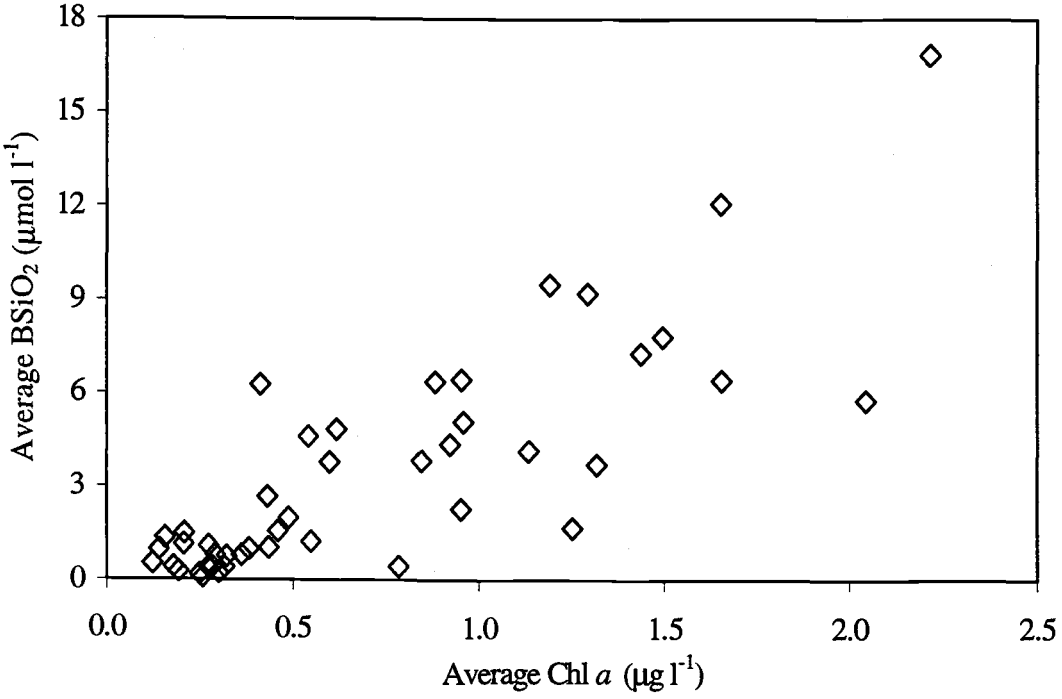

Fig. 9: Correlation of average $BSiO_2$ concentrations to average chl *a* concentrations for all profile stations

relationship. A highly scattered relationship between $BSiO_2$ and chl *a* indicates that either diatoms were not the always the dominant phytoplankton, or that this ratio is highly variable in Southern Ocean diatoms.

This analysis includes periods with very different $BSiO_2$:chl *a* ratios. In November, before the onset of the diatom bloom, $BSiO_2$:chl *a* averaged 1.9 μmol Si per μg chl *a* (s.d.= 0.55). By December, the ratio had increased to 4.7 μmol μg^{-1} (s.d.= 2.1), and by January it was up to 7.5 (s.d.= 4.3). By the March cruise, the $BSiO_2$:chl *a* ratio had decreased to 3.8 μmol μg^{-1} (s.d.= 3.0), likely in response to the loss of most of the diatom biomass between January and March. Most of the large variation in this ratio was due to changes in $BSiO_2$ concentrations. The range of chl *a* values encompassed a 10-fold range, whereas $BSiO_2$ concentrations varied by 100-fold. Therefore, small changes in chl *a* were correlated with large changes in $BSiO_2$, especially at higher chl *a* concentrations. Average euphotic zone $BSiO_2$:chl *a* ratios were also analyzed spatially, and were separated into two regions to the north and south of 60° S. The mean ratio of the 12 stations north of 60° S was 1.8 μmol μg^{-1} (s.d.= 1.2), whereas the mean of the 33 stations south of 60° S was 5.5 μmol μg^{-1} (s.d.= 2.8). Both of these $BSiO_2$:chl *a* ratios are extremely high, and do indicate that diatoms were the dominant phytoplankton both north and south of 60° S. However, the higher ratio south of 60° S indicates that either diatoms comprised a much larger fraction of phytoplankton biomass, or that the diatoms present had much higher $BSiO_2$:chl *a* ratios. This second scenario is most likely.

The extremely high $BSiO_2$ to chl *a* ratios south of 60° S could be explained by either diatoms producing cells with very little chl *a*, or a preponderance of dead diatoms remaining in the euphotic zone throughout the growing season. The second hypothesis is unlikely since we observed very high diatom biomass and very high Si production rates at many stations in December and January (Brzezinski et al. in press), which could only be explained by living diatoms. Additionally, high diatom biomass was observed below the mixed layer, with low but measurable rates of Si production at these depth. This scenario is indicative of sinking cells that are not effectively retained in the surface mixed layer, but are clearly still viable in the lower euphotic zone (see below). In other words, only in the lower euphotic zone, where $BSiO_2$ was generally much lower than at shallower depths, would the preponderance of dead diatoms be likely. Therefore, it is probable that

most of the diatoms encountered had very high $BSiO_2$, but very low chl *a* per cell, and that this effect was greater south than north of 60° S. It is likely that the higher $[Si(OH)_4]$ south of 60° S allowed the diatoms present to produce thicker frustules than diatoms to the north. A progression towards larger cell size south of 60° S would also lead to cells with more Si per cell, given that chl *a* per cell remained relatively unchanged. Both of these scenarios would lead to higher $BSiO_2$:chl *a* ratios south of 60° S.

Vertical gradients in $[Si(OH)_4]$ were observed in the euphotic zone during all but the first cruise, when no vertical structure in any Si parameter was observed. A vertical gradient existed only where $[Si(OH)_4]$ increased by >0.2 μM m^{-1} between any two sampling depths within the euphotic zone. The stations with average $BSiO_2$ >3.8 μmol l^{-1} typically had steeper vertical gradients in $Si(OH)_4$ concentrations than stations with lower $BSiO_2$ concentrations, and this gradient most often occurred between the 5% and 1% light depth. In December, $[Si(OH)_4]$ increased >10 μM between these light depths, and each of the 13 stations sampled in December at or south of 60° S revealed strong vertical $[Si(OH)_4]$ gradients within the euphotic zone. The average vertical Si gradient for all stations located between 60° and 65° S in December was 0.85 μM m^{-1} (range of 0.43-1.2 μM m^{-1}). By January, the maximal gradient had increased to ~30 μM between the 5% and 1% light depths (see Fig. 1). The average vertical Si gradient in January from 60° to 65° S was 1.45 μM m^{-1} (range 0.64-2.3 μM m^{-1}). However, there was one station sampled in January at 62° S that had no silicic acid gradient within the euphotic zone. $Si(OH)_4$ was stripped to <5 μM throughout the euphotic zone to a depth of 49 m, pushing the vertical Si gradient below the euphotic zone. Extremely high diatom biomass measured at this station in December most likely facilitated this scenario by shoaling the euphotic zone and by consuming $Si(OH)_4$ as some of the diatoms sank from the upper euphotic zone. The March cruise revealed remnant vertical $Si(OH)_4$ gradients, with maximal increases of ~20 μM $Si(OH)_4$ between the 5% and 1% light depth, even though Si production at this time was very low. When considering that diatom biomass and production rates were very low in March, it is very likely that the gradients observed at this time were remnants of $Si(OH)_4$ consumption during summer. There were strong vertical $Si(OH)_4$ gradients south of 60° S in each of the last 3 cruises, indicating strong

biological removal of Si in the upper euphotic zone, with net removal decreasing rapidly below the 5% light depth.

Analysis of the 12 profile stations that had an average $BSiO_2$ concentration >3.8 $\mu mol\ l^{-1}$ revealed that changes in Si production rates from ^{32}Si uptake experiments (reported in Brzezinski et al. in press) corresponded well with the observed vertical $Si(OH)_4$ gradients. In fact, 10 of the 12 stations had strong vertical gradients in Si production rates between the 5% and 1% light levels, with values severely declining by the 1% level. Furthermore, the steepest gradient in biomass-specific Si production rates in 7 of the 12 stations was located between the same light depths. Except for one station that displayed no gradients (see above paragraph) gradients in Si production rates at the remaining stations occurred between the 1% and 0.1% light depths. The diatoms observed in the lower euphotic zone were consuming little $Si(OH)_4$, and even when there was abundant $BSiO_2$ biomass present, the cells were not very productive below the 5% light depth. Therefore, biological rate estimates in high biomass stations generally decreased within or below the observed vertical $[Si(OH)_4]$ gradients. Accordingly, most of the diatom growth was occurring in the upper euphotic zone throughout the study area, and much of the $BSiO_2$ measured lower in the euphotic zone was likely due to sinking cells, not *in situ* production.

Mixed Layer Depth

Light and nutrient availability affect phytoplankton growth rates and abundance. In addition to biology influencing light and nutrient availability, physical processes also exert some control over these factors, primarily via mixing. Mixed layer depths (MLDs) were very important in allowing the extremely high diatom biomass to accumulate in the euphotic zone. The mixed layer is defined as the depth at which the density differs from the surface value by 0.01 $kg\ m^{-3}$, and these data were collected by J. Morrison and are listed at http://usjgofs.whoi.edu. During November MLD was >100 m throughout the study area, with the exception of the southernmost station at 62.4° S. That station was near the receding ice edge, and the mixed layer was likely stabilized by melt-water. In

fact, this was the only station sampled in November where the mixed layer was shallower than the euphotic zone, and it had with the highest integrated $BSiO_2$ concentrations and Si uptake rates measured during the November cruise (Brzezinski et al. in press). The mixed layer had shoaled to <40 m at all stations south of 56° S by December, with the exception of two stations within the APF where no Si rate measurements were performed. The shallower mixed layers were due to a combination of increasing surface temperatures, melting of sea ice, and decreased storm intensity, all of which are typical of the summer season as sunlight becomes more abundant. MLDs in January were comparable to conditions found in December, and were <50 m deep from 60° to 68° S. By March, mixed layer depths had deepened to >50 m within and north of the APF, and were <45 m south of the front, with the exception of the southernmost stations.

The shallowest mixed layers (<20 m) were closely associated with the receding ice edge in December and January. The melting of sea ice was very important in stabilizing the water column throughout spring and summer south of the Polar Front (Barth et al. in press). MLDs were shallowest at the southernmost station on all four cruises, the first three of which approached the sea ice on their southernmost stations. After November, the euphotic zone was always deeper than the mixed layer. The fact that diatoms were not being actively mixed out of the well-lit upper euphotic zone resulted in high $BSiO_2$ production rates, high $Si(OH)_4$ removal rates, and high accumulation of biomass, indicative of cells growing at near-optimal light intensities. The extreme shoaling of mixed layers in December and January probably aided in keeping the growing diatom cells in the surface layer longer, facilitating the accumulation of the highest open ocean $BSiO_2$ concentrations ever measured. The transition from January to March revealed increases in surface layer $[Si(OH)_4]$, decreases in $BSiO_2$, and deeper mixed layers, indicating strong vertical mixing that likely removed much of the diatom biomass out of the surface layer by vertical wind-forced mixing. Although the euphotic zone was still deeper than the mixed layer during this time period, low $[Si(OH)_4]$, deeper mixing and deteriorating light conditions associated with austral fall were likely responsible for the very low rates of activity of the diatom community at this time.

Biogenic silica production rates were also strongly dependent on the mixed layer depth within the main bloom area, between 61° and 65° S, in December and January. High absolute production rates (μmol Si l^{-1}) were observed only within the mixed layer in the bloom areas, and these rates dropped off significantly (generally by >50%) below the mixed layer. Specifically, in December and January, all stations with high $BSiO_2$ (>4 μmol l^{-1}), had the base of the high production surface layer within 5 m of the base of the mixed layer. Diatoms within the mixed layer were growing well, as evidenced by high production rates, but as cells sank below the mixed layer they were then confined to less favorable light conditions and, even though high biomass was often present, biological conversion of Si from $Si(OH)_4$ to $BSiO_2$ was very low and had likely become light-limited. This hypothesis is supported by the observation that vertical [$Si(OH)_4$] gradients were also generally associated with gradients in Si production rates, even though $BSiO_2$ concentrations in the core of the bloom areas were nearly uniform throughout the euphotic zone. Vertical gradients in [$Si(OH)_4$] and Si production rates generally occurred near the base of the mixed layer, and between the 5% and 1% light depth. Therefore, mixed layer depth < euphotic zone depth was very important in establishing optimal light conditions for the observed diatom blooms between 61° and 65° S.

Although MLD < EZD was necessary for significant accumulation of $BSiO_2$, there was no clear pattern relating the depth of the mixed layer to $BSiO_2$ or chl *a* concentrations. A regression analysis of average $BSiO_2$ concentration to MLD revealed a negative exponential function with an R^2 of 0.30, which is not significant at the 0.01 level. Regression analysis of chl *a* to MLD revealed a similar insignificant relationship ($R^2 = 0.24$). Regression analyses were also performed on integrated $BSiO_2$ and chl *a* concentrations, both of which confirmed insignificant relationships between the two biological parameters and the depth of the mixed layer. In fact, at stations where the shallowest mixed layers (<23 m) were observed in December and January, >50% of the diatom biomass was below the MLD. This indicates that MLD did not exert much control over the amount of production or biomass of diatoms within the euphotic zone. However, the data revealed that there was a threshold MLD above which diatom biomass was likely light limited. Only in mixed layers shallower than 65 m did >1.5 μmol Si l^{-1}, >0.6 μg chl *a* l^{-1}, and integrated $BSiO_2$ >150 mmol m^{-2} accumulate in the euphotic zone.

Effects of Physical Forcing

Advection and upwelling are two physical processes that can modify the observed trends in dissolved and particulate Si pools, as well as biological rate parameters. Eastward velocities of the ACC were highest within the APF, with mean velocities of ~0.2 m s^{-1}, and decreased both to the north and the south, with mean velocities south of the APF of ~0.05 m s^{-1} (Barth et al. in press). These estimates were similar throughout the study period, and can be used to address the effects of spatial and temporal patchiness and advection on the observed Si parameters. During December 1997, two stations located at 60.9° and 61.7° S were reoccupied 11 and 9 days after initial sampling, respectively. Using the above rates of horizontal advection, the water initially sampled at 60.9° S would have traveled 190 km eastward, and at 61.7° S would have traveled 39 km eastward by the time the ship reoccupied each station. Satellite sea-surface images of chl *a* from the Southern Ocean indicate small and large scale patchiness in chl concentrations in this area (Moore et al. 1999). It is possible that the reoccupation of the same site sampled parts of a very large patch, or that two unique but similar patches were sampled. Regardless of the scale of patchiness, the observed drawdown of $Si(OH)_4$ and export of $BSiO_2$ in the study area is rather insensitive to patches of $BSiO_2$. Nutrient concentrations indicate large scale depletion of $Si(OH)_4$ throughout the study area. Additionally, instantaneous measurements of $BSiO_2$ represented only a small fraction of $Si(OH)_4$ removal, and hence total Si export. Thus, incorporation of occasional unrepresentative patches of $BSiO_2$ that were being advected through this system would not significantly affect total Si export estimates

The station within the APF, at 60.9° S, had similar $Si(OH)_4$ and $BSiO_2$ concentrations during both samplings. Surface [$Si(OH)_4$] were 13.6 and 13.9 μM, while integrated [$Si(OH)_4$] were 900 and 685 mmol m^{-2} and integrated $BSiO_2$ concentrations were 423 and 433 mmol m^{-2}, for the first and second sampling respectively. Therefore, although the area within the front is very dynamic with high advection rates, the diatom biomass and surface layer [$Si(OH)_4$] were very similar, indicating a reasonably large scale of elevated biomass within the APF. Furthermore, 6 stations were sampled within the APF jet (60.3-61.2° S) over 12 days during December, with a mean $BSiO_2$

concentration of 440 mmol m^{-2} (s.d.= 79). The relatively consistent $BSiO_2$ concentrations indicate high diatom biomass throughout the APF, and even high rates of horizontal advection of latitudinal variations in frontal circulation could not mask the biological signal. However, integrated $[Si(OH)_4]$ did reveal the dynamic nature of the front, with concentrations in the upper 50 m ranging from 620 to 930 mmol m^{-2}. The variations in $Si(OH)_4$ were likely due to upwelling and downwelling associated with meandering of the APF (Barth et al. in press).

At 61.7° S, significant changes in both $[Si(OH)_4]$ and $BSiO_2$ were observed in the 9 days between samplings. Integrated $[Si(OH)_4]$ dropped from 1890 to 860 mmol m^{-2} and $BSiO_2$ declined from 790 to 392 mmol m^{-2}. The importance of the decreases in $[Si(OH)_4]$ at this location is obvious when considering that the only way that $Si(OH)_4$ will decrease in a water parcel is by biological uptake. It is highly unlikely that the reoccupation at 61.7° S could have sampled the same patch since total surface layer Si had decreased by >50%, which would be an extremely high Si loss rate (~1.3 mol Si m^{-2} in 9 days). Therefore it is likely that the patch sampled the second time was advectively transported into the same geographical position, and that significant diatom Si uptake had taken place in that water mass. This also indicates large scale diatom production throughout the region. Thus, advective transport can influence and skew instantaneous parameter measurements from total system means, but it cannot mask the fact that significant biological activity was proceeding throughout the APF and southern ACC. Since resupply is continually occurring in the ACC, biological drawdown is the only process that could explain the consistent and widespread removal of $Si(OH)_4$ observed throughout the ACC from November to January.

The Southern Ocean is a general area of upwelling due to differential wind stress with latutiude. Comiso et al. (1993) estimated average wind-driven upwelling rates between the APF and the SACCF of 2-2.5 x 10^{-5} m s^{-1}, or 1.7-2.2 m d^{-1} on an areal basis (~2 m^2 d^{-1}). This upwelling therefore implies that ~2 m of water from below the mixed layer is being injected into the surface layer on a daily basis. Vertical gradients in $[Si(OH)_4]$ are consequently very important in determining the supply of $Si(OH)_4$ to the surface layer via upwelling. In November, there were no vertical gradients in $[Si(OH)_4]$ within the upper 100 m south of the APF. Therefore, upwelling in early spring was not

injecting any higher concentration $Si(OH)_4$ water into the surface layer. However, by December there were strong vertical gradients in $[Si(OH)_4]$ observed at all 13 stations between 60° and 65° S (see above). All of the gradients occurred within the euphotic zone and at the base of or below the surface mixed layer (see Appendix for station profile information). Interestingly, 9 of the 13 stations had the steepest $[Si(OH)_4]$ gradients 10 or more meters below the base of the mixed layer. The fact that the maximal vertical $Si(OH)_4$ gradients did not coincide with the MLD indicates that Si uptake by diatoms was proceeding below the mixed layer faster than the rate of resupply via dissolution, upwelling, mixing, and advection. The depth of the steepest vertical $Si(OH)_4$ gradients at most stations also implies that $Si(OH)_4$ supply via upwelling was of minor importance in December since water upwelling into the mixed layer, from the lower euphotic zone, would already be low in $Si(OH)_4$, and similar to concentrations at shallower depths.

There were smaller but measurable vertical gradients in $[Si(OH)_4]$ at or just below the mixed layer at all 13 stations in December. The mixed layer gradient was determined by the difference in $[Si(OH)_4]$ across the base of the mixed layer (i.e. two depths sampled on each side of the MLD) or between the base of the mixed layer and the next sample depth (used when a sample depth was within 1 m of the MLD). In December, the mean vertical $Si(OH)_4$ gradient across the mixed layer between 60° and 65° S was 0.31 $\mu M\ m^{-1}$ (or mmol m^{-4}). This value is 37% of the average maximal vertical $Si(OH)_4$ gradient in December (occurring below the MLD). It is the gradient across the MLD that will be used in calculating supply of $Si(OH)_4$ into the mixed layer due to upwelling. Given the mean upwelling rate of 2 $m^2\ d^{-1}$, an average of 0.62 mmol Si $m^{-2}\ d^{-1}$ was being added to the mixed layer in December. By January, the maximal vertical Si gradients were much steeper, while MLD were similar (see above). However, there were only 5 station profiles performed in this region during January. The two stations located around 65° S had maximal vertical $[Si(OH)_4]$ gradients coincident with the mixed layer gradients, with $[Si(OH)_4]$ gradients at each station of ~2.5 mmol m^{-4}, resulting in a daily influx of 5 mmol m^{-2}. The three stations north of 65° S had much lower gradients (mean of 0.13 mmol Si m^{-4}), resulting in supply rates of 0.26 mmol Si $m^{-2}\ d^{-1}$ due to upwelling. Given that the average of rate of $Si(OH)_4$ removal from November to January was 27.5 mmol $m^{-2}\ d^{-1}$, the supply of $Si(OH)_4$ via upwelling would typically represent <3% of net

drawdown (~9% at 65° S in January). Therefore, it appears that vertical resupply of $Si(OH)_4$ to the surface layer was very small in comparison to biological uptake during the peak of the growing season. Even if the maximal $Si(OH)_4$ gradient values were used, the contribution from upwelling would only account for <10% of the average daily removal rate of $Si(OH)_4$.

Export from the surface layer includes both biological and physical processes. Passive sinking of diatom cells was evident throughout December and January within and south of the APF. Heavily silicified diatoms formed in the upper euphotic zone will have a tendency to sink to greater depths, creating a vertically extended area of high biomass which extends deeper than the area of high uptake rates (see above for discussion of production rates within mixed layer). The scenario of elevated yet unproductive $BSiO_2$ concentrations below the mixed layer, was seen in all stations with >4 μmol l^{-1} average $BSiO_2$ during both summer cruises. Therefore, this process was common through much of the ACC in summer. Vertical advection was also evidenced to export biogenic particles. During austral spring, a layer of cold, dense surface water moving northward was being subducted beneath the APF (Barth et al. in press), and was also evident in early December. A high $BSiO_2$ signal was associated with the subduction of the colder, denser layer beneath the APF. However, this feature was not evident in late December or January, likely due to the warming of the surface layer and melting of sea ice, which prevented its density-driven subduction. Wind induced mixing was also observed to transport $BSiO_2$ out of the surface layer. The largest and most spatially extensive change in $BSiO_2$ occurred between late January and mid-February from 61° to 65° S, due to increased vertical mixing which deepened the mixed layer (see above discussion of mixed layer depths). This event not only exported considerable amount of $BSiO_2$ from the surface layer, it also marked the end of the growing season, as evidenced by essentially no net silica production in March (Brzezinski et al. in press).

DISCUSSION

Changes in surface layer [$Si(OH)_4$] and $BSiO_2$

Silicic acid and its dissociation products, all of which are measured in the standard colorimetric analysis (Strickland & Parsons 1972), account for nearly 100% of dissolved Si in seawater (Stumm and Morgan, 1981). Particulate silica occurs only in biogenic and lithogenic forms, and both forms are readibly and commonly measured (Nelson & Brzezinski 1997). Therefore all forms of Si can be measured, making the biogeochemical cycle of Si in the ocean relatively simple compared to other nutrient cycles. Lithogenic silica concentrations during this study were generally <4% of total particulate Si in the euphotic zone, and therefore contributed very little to particulate Si concentrations. Consequently, the components of the Si cycle can be further simplified into $Si(OH)_4$ and $BSiO_2$, which comprise ~100% and ~95% of the dissolved and particulate Si pools, respectively, in this study. Therefore, interpretations of changes in any component of the Si cycle are more robust than if other unknown or unquantified forms of the element existed, such as dissolved organic Si.

The southern edge of the APF was located between ~60° and ~61.5° S throughout most of the sampling period. The steepest horizontal gradient in [$Si(OH)_4$] was initially located within the APF in spring, but propagated further south through summer. $Si(OH)_4$ removal in the upper 80 m propagated southward from November to January as the edge of the sea ice retreated, creating a stronger meridional gradient in the process. In November the [$Si(OH)_4$] gradient increased ~12 μM over 1° latitude (increasing to the south). By January, the gradient had been shifted much further south and was compressed significantly due to biological removal of $Si(OH)_4$. The gradient in January was centered at 65° S, where surface [$Si(OH)_4$] increased >25 μM over 1° latitude. Silicic acid concentrations were depleted to <2 μM in near-surface waters down to 64.5° S over this time. Most removal was confined to the upper 40-60 m, with deepest removal observed north of 62° S.

Net removal of $Si(OH)_4$ from the surface layer was greatest between December and January, with maximal removal rates of ~1.0 μM d^{-1}. These high removal rates were confined to the upper 40 m between 61° and 65° S. The removal rate of 1.0 μM d^{-1} is ~75% of maximal gross Si production rates based on ^{32}Si experiments measured in the peak of the bloom (Brzezinski et al. in press). Therefore, net $Si(OH)_4$ drawdown is consistent with the measured uptake of $Si(OH)_4$ and subsequent production of $BSiO_2$ by diatoms in this area. Based on changes in integrated [$Si(OH)_4$] between 61° and 65° S, an average of 2,200 mmol Si m^{-2} was removed from the upper 50 m between November and January, corresponding to an average [$Si(OH)_4$] decrease of 43 μM. In comparison, nitrate concentrations in the upper 50 m during that time only decreased by ~6 μM in the same area (Morrison et al. in press). Therefore, net seasonal drawdown of $Si(OH)_4$ was ~7 times greater than the net drawdown of nitrate in the same area, indicating very high Si:N export ratios in this area of the Southern Ocean. Nearly all (99%) of the seasonal net $Si(OH)_4$ removal had occurred in the study area by late January, and by March significant amounts of $Si(OH)_4$ had been resupplied to the system, primarily via mixing with nutrient-rich subsurface waters. There was no net $Si(OH)_4$ drawdown during March over most of the study area (Brzezinski et al. in press). $Si(OH)_4$ resupply via frustule dissolution, mixing, and upwelling is continually occurring in most of the Southern Ocean, but the biological uptake of $Si(OH)_4$ by diatoms was much greater than the sum of the resupply terms between November and January. The decreases in biological uptake late in the growing season, combined with more intense wind-driven mixing in early February, caused the supply of $Si(OH)_4$ to the surface layer to exceed biological demand.

Biogenic silica concentrations and changes corresponded well with both vertical and horizontal [$Si(OH)_4$] gradients. However, the largest magnitude and spatial extent of increase were observed in December, whereas most of the $Si(OH)_4$ removal was observed between December and January. Biogenic silica accumulated in significant amounts only south of 61° S, and was therefore constrained to areas that had initial [$Si(OH)_4$] >20 μM. The highest integrated $BSiO_2$ concentration of 700 mmol m^{-2} was at 62° S in December, whereas the highest concentration by volume of 17 μmol Si l^{-1} was measured at 65° S in January. The high $BSiO_2$ concentrations measured during December and January are the highest open ocean values ever measured. Maximal $BSiO_2$ accumulation rates observed

during the study period were 0.3 μmol Si l^{-1} day^{-1}, or about one-third of the observed maximal $Si(OH)_4$ removal rates. This finding is consistent with the fact that not all $Si(OH)_4$ removal is retained as $BSiO_2$ in the surface layer due to vertical export from the euphotic zone. The large spatial and temporal coverage of the diatom bloom region is illustrated by concentrations of $BSiO_2$ >475 mmol m^{-2} during the height of the growing season (December to January) at all latitude bands between 61° and 65° S. Therefore, areas with the largest removal of $Si(OH)_4$ also had the highest $BSiO_2$ concentrations, as is expected since removal is entirely biological in the surface ocean.

Euphotic zone depth is very relevant to diatoms, since photosynthetic organisms are dependent on the ambient light conditions, and not the absolute depth at which they are located. The clear relationship between $BSiO_2$ concentrations and EZD indicates that diatoms can exert a significant control over light penetration through the water column. This pattern is also expected, since diatoms contain chl *a* and other light-harvesting pigments. However, it is interesting to note that $BSiO_2$ exerted a greater control on EZD than did chl *a*, and indicates the dominance of the phytoplankton community by diatoms. Furthermore, the $BSiO_2$:chl *a* ratios were extremely high south of 60° S, averaging 5.5 μmol Si (μg chl *a*) $^{-1}$. This ratio is also consistent with the observation that Si removal from the surface layer was much greater than N removal. The relatively poor correlation between $BSiO_2$ and chl *a* can be explained by 2 scenarios. One is that diatoms do not dominate phytoplankton biomass, and would therefore not vary with chl *a* concentrations. Another possible explanation is that diatoms in the Southern Ocean have very little chl *a* per cell. This scenario could result from very high $BSiO_2$:chl *a* ratios in living diatom cells, or if much of the measured $BSiO_2$ biomass is not viable. Due to its transient nature, chl *a* is only found in live or viable cells, while $BSiO_2$ remains well after the cell has died and can therefore be abundant in the water column, even with few live diatoms. It is clear from Si removal and production rates, and the high $BSiO_2$:chl *a* ratios that the measured diatoms indeed had low cellular chl *a* content. However, it is also clear that there were several stations that had high $BSiO_2$ concentrations, especially at greater depths, but low Si uptake rates, indicating an abundance of dead or dying diatoms in the lower euphotic zone. Therefore, it is likely a combination of dead cells and low cellular

chl *a* that results in the extremely high $BSiO_2$:chl *a* ratios of the phytoplankton community.

There was very little change in $Si(OH)_4$ or $BSiO_2$ with depth below 100 m between November 1997 and March 1998, while rate estimates of diatom production and growth began to drop rapidly with depth by 60 m. In fact, most $Si(OH)_4$ drawdown occurred within the upper 40-50 m south of the APF (see Fig. 1). Furthermore, during November there was only one station where the euphotic zone was deeper than the mixed layer, whereas through the rest of the sampling period, MLD was always < EZD. In November, deep mixed layers effectively prevented diatoms from accumulating significant biomass by mixing them deeper than the euphotic zone, thus transporting cells to depths where light was limiting. By December, active mixing had decreased significantly, allowing phytoplankton cells to remain in the well-lit surface waters. These findings indicate biological mediation of [$Si(OH)_4$] in the surface layer, and physical control at greater depths. Thus, diatoms were able to consume $Si(OH)_4$ and convert it to $BSiO_2$ only in the well-lit surface waters where photosynthesis can take place. Below the euphotic zone, diatoms can no longer grow, and therefore cannot take up $Si(OH)_4$. Located in the general area of upwelling within the ACC, the area south of the APF, at ~61° S, is continuously being resupplied with $Si(OH)_4$. Therefore, silicic acid should decrease only in regions where uptake exceeds supply through dissolution and upwelling. This situation appears to be confined to the upper euphotic zone.

When present within the euphotic zone, strong vertical gradients in [$Si(OH)_4$] were commonly located between the 5% and 1% surface-incident light depth at all stations with high $BSiO_2$ concentrations. These gradients appear to be caused by gradients in biological rate parameters, and not by physical processes, such as the depth of the mixed layer or the rate of upwelling. At most of these stations, absolute Si production rates and diatom growth rates dropped rapidly between the 5% and 1% light depths (Brzezinski et al. in press). Therefore, significant diatom uptake of Si did not normally extend to depths greater than the 5% light depth. Even though there was often significant biomass present at greater depths, the measured production rates of $BSiO_2$ by the diatoms at these depths were very low. A likely explanation for these observed trends is that high diatom biomass accumulated in the well-lit surface waters (above the 5%

light depth), and then sank through the water column to greater depth. Interestingly, even the relatively low Si uptake rates of the sinking diatoms in the lower euphotic zone moved the maximum vertical [$Si(OH)_4$] gradients below the MLD. In general, uptake rates in the lower euphotic zone were ~10% of rates in the upper euphotic zone. Supply of $Si(OH)_4$ via upwelling only contributed <3% of average surface layer $Si(OH)_4$ removal between November and March. Therefore, even at sub-optimal light conditions, the uptake of the high $BSiO_2$ biomass measured throughout 61° to 65° S in December and January was enough to consume and therefore mask the $Si(OH)_4$ inputs via upwelling. This biological uptake at depth effectively prevented any high [$Si(OH)_4$] water from being injected into the mixed layer, and therefore allowed near-surface concentrations to be stripped by an average of 43 μM.

It is clear that the depth of the mixed layer was crucial in allowing the formation of the observed diatom blooms. Only at stations where MLD < 65 m did significant chl *a* or $BSiO_2$ accumulate. However, neither biological biomass parameter was significantly correlated with MLD. Shoaling of the mixed layer occurred in response to increased insolation which warmed the surface layer and melted sea ice. These stabilizing processes, in combination with decreased storm intensity, confined the diatoms to the upper euphotic zone in near-optimal light, thus facilitating a diatom bloom. As biomass increased, cells slowly sank out of the mixed layer, while still consuming $Si(OH)_4$, though at a much lower rate, throughout the lower euphotic zone. This process continued until an average of >80% of the initial [$Si(OH)_4$] was removed from the upper 50 m in the study area north of 65° S.

Export from the surface layer

Changes in vertically integrated $BSiO_2$ and [$Si(OH)_4$] can be used to estimate the fraction of net $Si(OH)_4$ consumption that is still present in the euphotic zone as $BSiO_2$. A seasonal average of 17% of $Si(OH)_4$ removal was measured as $BSiO_2$ accumulation in the euphotic zone. This relationship does not consider the actual concentration of $BSiO_2$ at the time of sampling, only the accumulation of $BSiO_2$ between cruises within the same

latitude band. There were differences in the ratio of removal to accumulation within the growing season. As would be expected in spring bloom scenarios, a greater proportion of $Si(OH)_4$ decrease was retained in surface waters as biogenic silica accumulation early in the season. Specifically, ~30% of $Si(OH)_4$ removal observed between November and December remained as accumulated $BSiO_2$ in the euphotic zone. However, much less (~10%) of the observed $Si(OH)_4$ depletion between December and January was measured as an increase in $BSiO_2$. This is due to a combination of differences in removal and accumulation over this time period. The fact that high diatom biomass was already present in the surface layer minimized the observed net accumulation of $BSiO_2$ between December and January. In addition, much more $Si(OH)_4$ was removed between December and January, suggesting greater export of $BSiO_2$ from the surface layer in summer via advection or sinking (including grazing or aggregation). Export of $BSiO_2$ at 100 m was also greater later in the growing season (Buesseler et al. in press). Greater nutrient removal relative to accumulated biomass is also consistent with spring bloom scenarios, as heterotrophic processes and nutrient depletion often lead to increased export later in the growing season.

Total Si in the upper 50 m of the bloom region from 61° to 65° S decreased by an average of 2,000 mmol m^{-2} between November and January, and provides our best estimate of net Si export from the surface layer. Of the seasonal export, 1,150 mmol Si m^{-2} or 57% occurred between December and January. The large Si export in less than 80 days indicates that diatom biomass rapidly sinks out of the surface layer, for $BSiO_2$ export is the only loss term for Si in the system. Si export from the surface layer based on these mass balance calculations represented an average of 71% of the initial Si present in the surface layer between 58° and 65° S (see Fig. 6). Conversely, these calculations indicate that <30% of the $BSiO_2$ produced in the euphotic zone dissolved in the upper 50 m. Therefore, the Southern Ocean north of 66° S is a highly efficient Si exporting system, with most of the surface layer Si being exported via diatom production in less than 3 months.

The magnitude of the seasonal Si export estimates (given in Table 3), based on changes in Si pools, are minimum estimates of the annual export. The above analysis considers only net seasonal changes in the dissolved and particulate pools that were

actually observed between the first and last cruise. Therefore, $Si(OH)_4$ removal and $BSiO_2$ production before November or after March are not quantified or included in this analysis. Furthermore, $Si(OH)_4$ consumption is not quantified between late January and March, due to the net resupply of $Si(OH)_4$ in the surface layer, even though Si uptake was occurring (evidenced by low Si uptake rates, Brzezinski et al. in press). Silicic acid was also being resupplied to the surface layer through *in situ* dissolution of diatom frustules, and added through upwelling and episodic mixing from below the mixed layer, each of which causes the observed net drawdown to be lower than gross $Si(OH)_4$ removal. Similarly, the estimates of $BSiO_2$ changes do not account for periods of continued production and sinking that result from continuing of diatom growth. In other words, diatoms were being produced and sinking out of the surface layer throughout the study period, but only instantaneous biomass was measured, and net changes in the euphotic zone biomass calculated. However, we can safely assume that no more than 10% of annual $BSiO_2$ production between 58° and 68° S occurred outside of our sampling period. This assumption is based on very low rates of Si production throughout this area in both November and March and on low surface layer [$Si(OH)_4$] observed in March. Both of these factors indicate that very little production and hence export could occur outside of the growing season.

Using an average dissolution rate of 6.5 mmol Si m^{-2} d^{-1} (given by Brzezinski et al. in press) results in >500 mmol Si m^{-2} being resupplied to the euphotic zone between November and January. Dissolution of *in situ* $BSiO_2$ does not affect the net export estimates, for dissolution is only recycling Si that was included in the initial total Si of the system. This rate of dissolution would account for >180 mmol m^{-2} of $Si(OH)_4$ resupplied to the euphotic zone in the time between the January and March cruises, therefore accounting for most of the observed resupply between 58° and 68° S (Table 1). Given that deep mixing did occur during this time period (based on increased mixed layer depths), the observed increases in [$Si(OH)_4$] resulted from the difference in dissolution + upwelling + mixing - biological uptake. In other words, biological uptake of $Si(OH)_4$ was occurring during this time period, but the physical processes resupplying the Si masked much of the biological signal.

The only factors that would significantly affect the net export estimates are upwelling and espisodic mixing, both of which bring deeper, nutrient-rich water into the surface layer. As mentioned previously, upwelling from within surface mixed layer or even the lower euphotic zone would increase the observed drawdown of $Si(OH)_4$ by <10%. Therefore, it is safe to say that upwelling could maximally increase Si export estimates by <10%, and likely <5%, and this effect is limited to the upwelling region of the southern ACC (61° to 65° S). The largest unknown is episodic mixing events. However, one can conservatively assume that a surface mixing event that entrains 10 m of water from below the mixed layer occurs once during both the December and January cruises. Each mixing event would therefore supply, on a monthly basis, ~20% of the $Si(OH)_4$ supplied via upwelling, given the depth and magnitude of the observed $Si(OH)_4$ gradients. Therefore, our estimates of Si export would at most be underestimated by ~12% in the southern ACC, and less than this in regions to the north and south. Nonetheless, the area of the Pacific sector of the Southern Ocean between 61° and 65° S has high $Si(OH)_4$ removal and $BSiO_2$ production and export, and is likely responsible for the opal-rich sediments found beneath the southern ACC. This conclusion was also reached by Pondaven et al. (2000) in the Indian sector of the Southern Ocean.

Comparisons to Other $BSiO_2$ Production Estimates

The estimates of $Si(OH)_4$ removal presented here compare very well with estimates of gross $BSiO_2$ production in the same area over the same time period. Gross Si production rates represent the rate at which $Si(OH)_4$ is converted to $BSiO_2$, before dissolution. Estimates of gross $BSiO_2$ production between 62° and 65°S, based on ^{32}Si uptake experiments, averaged 2,960 mmol m^{-2} (Brzezinski et al. in press), compared to 2,350 mmol m^{-2} of net $Si(OH)_4$ removed from the upper 50 m. Assuming a constant dissolution rate of 6.5 mmol Si m^{-2} d^{-1} (given in Brzezinski et al. in press) for the 80 days during which the seasonal drawdown was calculated, then net $BSiO_2$ production (gross production - dissolution) calculated from tracer experiments would be 2,440 mmol Si m^{-2}. This estimate of net $BSiO_2$ production obtained from tracer experiments is

indistinguishable from the estimate based on observed net $Si(OH)_4$ removal given the uncertainties inherent in vertical integration of Si standing stock and rate parameters. Furthermore, the gross $Si(OH)_4$ uptake estimate is integrated to the base of the euphotic zone, and therefore includes areas of both high and low rates of Si uptake and dissolution. Our net Si removal estimate is confined to the upper 50 m, where most of the $Si(OH)_4$ removal occurred, but obviously misses some areas of measurable drawdown. What is clear from this comparison is that measured rates of Si uptake are of almost exactly the right magnitude to support the observed removal of $Si(OH)_4$ from the upper 50 m. Therefore, it is our conclusion that both methods have accurately described the large scale removal of $Si(OH)_4$ from the surface layer of the Southern Ocean.

Another comparison of $Si(OH)_4$ removal rates and the subsequent production and export of $BSiO_2$ has been made with data collected in the Indian sector of the Southern Ocean. Pondaven et al. (2000) constructed a similar Si budget based on seasonal $[Si(OH)_4]$ data over a 90 day growing season. As was discovered in our study, the geographical region which showed the most net $Si(OH)_4$ drawdown was located just south of the APF. They estimated that 2,310 mmol Si m^{-2} was removed from the surface layer of this region during the summer growing season. Our estimates of $Si(OH)_4$ removal in the region just south of the APF (62°-65° S) were 2,350 mmol Si m^{-2}. These estimates are nearly identical, which is surprising given the different hydrographic regimes south of the APF in the Pacific and Indian sectors. In our study area the seasonal ice zone approaches the APF, whereas in the Indian sector, there is a large area of permanently open ocean between the APF and the seasonal ice zone. Therefore, the Pacific sector is seasonally influenced by melt-water stratification associated with the retreating ice edge. It is believed that this process is paramount in shoaling the surface mixed layer and facilitating diatom bloom formation. However, the Indian sector has no such mechanism for stabilizing and shoaling the mixed layer. Yet, it is apparent that in both regions seasonal diatom growth removes similar and large amounts of $Si(OH)_4$ from the surface layer via $BSiO_2$ formation, and that this material is exported to depth.

A comparison of the various surface layer $BSiO_2$ export estimates discussed above are presented in Table 4. The 50 m export estimates are taken from this study, and are given as export based solely on net $[Si(OH)_4]$ removal and as net total Si removal

Table 4: Seasonal production and export of $BSiO_2$ in the region just south of the Antarctic Polar Front (in mol m^{-2})

Estimate Method	Latitude Range (°S)	Net $BSiO_2$ export
Total Si budget (50 m) (this study)	62-65	**2.11**
$[Si(OH)_4]$ depletion (50 m) (this study)	62-65	**2.35**
Si production rates (Brzezinski et al.)	62-65	**2.4**
$[Si(OH)_4]$ depletion (~100m) (Pondaven et al.)	51-58	**2.31**
	Annual Global Average	**0.35**

(includes $BSiO_2$). The net $BSiO_2$ export estimates, based on production and dissolution rates, are for the euphotic zone (Brzezinski et al. in press). The 100 m export in the Indian sector (Pondaven et al. 2000) are based solely on net $[Si(OH)_4]$ removal compared to winter values. As previously mentioned, all of these estimates of export are very similar. Regardless of the hydrodynamic differences between the Indian and Pacific sectors, it is clear from both studies that the zone of the ACC directly south of the APF supports the highest production and export of $BSiO_2$ in the open Southern Ocean.

Nelson et al. 1995 estimated the global mean rate of gross $BSiO_2$ production to be 700 mmol m^{-2} y^{-1}, and that the mean Southern Ocean production rate is very similar to the global mean. Nelson et al. (1995) also estimated that globally >50% of this production dissolves in the upper 100 m. Therefore, net Si removal, and thus average $BSiO_2$ export from the upper 100 m would be ~350 mmol m^{-2} y^{-1} on a global basis, and this value is also presented in Table 4. Thus, the hydographic region of the ACC just south of the APF supports net seasonal $BSiO_2$ export that is 6-7 times greater than the global annual average in both the Pacific and Indian sectors. These high rates of export over such a short, but similar, growing season indicates that high export is occurring in the southern ACC throughout the Southern Ocean. This conclusion is also supported by the fact that low $[Si(OH)_4]$ was observed everywhere north of 65° S by January, within the eastward flowing ACC. More specifically, since the generally zonal flow of the ACC supplies water from the west, the consistently low $[Si(OH)_4]$ observed indicates that similar amounts of removal, and thus export, had occurred throughout the southern ACC.

It is apparent that the southern ACC, a region of general upwelling, supports unusually high rates of $BSiO_2$ production and export from the surface layer. Si export estimates from both the Pacific and Indian sectors of the Southern Ocean indicate that annual export is occurring at 6-7 times the global mean. Although the hydrographic regimes may be different, the observed high rates of $BSiO_2$ production and export from the surface layer appear to only occur in the southern ACC. This region of the ACC is bounded on the north by the APF, which typically has a winter $[Si(OH)_4]$ gradient associated with it. Therefore, there are two factors that are common throughout the southern ACC- seasonally high (>50 μM) $[Si(OH)_4]$ and generalized upwelling. What ever the cause, it is clear that this region of the Southern Ocean supports the largest global open ocean Si export from the surface layer in both magnitude and spatial extent. It is this production and export that appear to be the main factors responsible for the observed circumpolar siliceous sediments underlying the southern ACC. The connection between high $BSiO_2$ production in and export from the surface layer to deep sea fluxes and sediment accumulation will be discussed in the next chapter.

Chapter 3:

Coupling of the Surface Si Cycle to Si Flux and Burial

The surface layer Si cycle of the Southern Ocean along 170° W was studied extensively over an entire growing season from late October 1997 to mid-March 1998. This was the first comprehensive project that measured all components of the surface layer Si cycle, $BSiO_2$ production rates, and $BSiO_2$ dissolution rates in the open Southern Ocean. In addition, there were many other parameters measured concurrently with our own, including measurements of biological processes and standing stocks, chemical constituents, and physical forcing, some of which were discussed in the previous chapter. Several other investigators measured components of the Si cycle below the surface layer. Estimates of $BSiO_2$ flux and export were made for the upper 100 m (Buesseler et al. in press), the upper 1000 m (Honjo et al. 2000), and the entire water column (Sayles et al. in press). This chapter will relate our estimates of $BSiO_2$ export out of the surface layer to these other estimates of flux and export.

Total Si export estimates can be compared to particle flux estimates made on similar time and space scales. Flux of $BSiO_2$ out of the upper 100 m was estimated using ^{234}Th (Buesseler et al. in press). This isotope is produced at a constant rate by the decay of ^{238}U, and is typically scavenged from seawater by particles, while ^{238}U is conservative. Therefore, decreases in the ratio of ^{234}Th to ^{238}U in the upper 100 m can be used to estimate particle flux (Buesseler et al. in press). Ratios of ^{234}Th to $BSiO_2$ on filters were used to extrapolate to $BSiO_2$ flux. The ^{234}Th flux data were obtained on each of the four cruises, and therefore these estimates of export can be directly compared to our estimates, made on the same water mass during the same time period. Sediment trap collections were used to estimate $BSiO_2$ fluxes to 1,000 m (Honjo et al. 2000). Unfortunately, the sediment trap data record ended in January 1998, and therefore did not cover all of our sampling period. In fact, the majority of sediment trap data were from the previous growing season (1996-97). However, there is a record for over an entire annual cycle of fluxes. Assuming that fluxes are comparable from year to year and that the seasonal

patterns of production and flux are similar interannually, sediment trap fluxes can be used for comparison to our surface layer export estimates. $BSiO_2$ flux to the seabed and burial in the sediments were also measured at various stations throughout the study area via benthic landers and sediment samples (Sayles et al. in press). Estimates of Si burial in sediments consider much longer time scales than processes measured in the water column, and therefore represent a long-term mean burial rate. In order to compare all flux rates, each estimate was extrapolated to annual rates of mmol Si m^{-2} by each investigator (detailed methodology given in Nelson et al., this issue). However, our estimates of Si export from the upper 50 m are based on seasonal changes in total Si, and therefore provide only a seasonal estimate of export since no constraints have been placed on Si production from time periods outside our cruises. However, based on low Si production rates in November and March (Brzezinski et al. in press) and low $[Si(OH)_4]$ in surface waters by March, we can safely project that most of the production and export of $BSiO_2$ occurred during our sampling period. Therefore, our seasonal estimates of Si export are assumed to be essentially equivalent to annual rates.

There were four sediment traps moored in the study area. The sediment traps were located at 56.9°, 60.2°, 63.2°, and 66.1° S. The locations of the traps were such that each trap was located in a different hydrographic regime. The northernmost station was located north of the APF in sub-Antarctic waters. The station at 60.2° S was located within the APF region, and specifically within the APF jet. The station at 63.2° S was located approximately halfway between the southern edge of the APF and the northern edge of the SACCF. The southernmost station was located south of the SACCF in Ross Sea Gyre water. Therefore, all Si export estimates between 55° and 68° S were placed into four latitudinal bins, which spanned each mooring, and were located in different hydrographic regimes. All stations or latitude bands within a zone were averaged to obtain mean $BSiO_2$ flux rates for each hydrographic zone. The northernmost latitude range was the sub-Antarctic zone (55-58° S), the next was the APF zone (59-61° S), the third was the southern ACC zone (62-65° S), and the fourth was the Ross Sea Gyre zone (66-68° S).

The Si export estimates for the described regions are presented in Table 5. Our estimates of Si export from the upper 50 m reveal that the southern ACC zone had the

Table 5: Comparison of $BSiO_2$ fluxes based on changes in total surface layer Si, ^{234}Th fluxes, sediment trap data, flux to and burial in the seabed (all in mmol Si m^{-2})

Latitude Range (°S)	Mooring	Southern Ocean subsystem	Seasonal export (50 m)	Annual Th-based export (100 m)*	Annual sediment trap flux (1000 m)*	Annual flux to seabed*	Annual Si burial in sediments*	% of 50 m export reaching 1000 m
55-58	M2	sub-Antarctic	316	640	281	284	16	89
59-61	M3	PFZ	878	1420	379	337	48	43
62-65	M4	southern ACC	2109	1400	940	1325	163	45
66-68	M5	RS Gyre	513	340	206	252	16	40

* given in Nelson et al. (in press)

highest export rates. All other flux estimates of Si, including 100 m, 1000 m, seabed fluxes, and burial in the seabed, confirm that $BSiO_2$ export was greatest in this zone. In fact, the estimates of Si export from 50 m, flux estimates to 1000 m and the benthos, and Si burial estimates were more than twice as high in the southern ACC than in any other hydrographic zone. Most of the southern ACC along 170° W is seasonally covered by sea ice, and it is this region where diatom biomass and production was greatest. Export based on ^{234}Th fluxes indicated equally high values within the APF and the southern ACC, and both of these regions were more than twice as great as export estimates to the north or south. Si fluxes in the sub-Antarctic zone and the Ross Sea Gyre zone were very similar within each type of flux estimate, and represented the lowest Si export fluxes in the study area. In general, the 50 m, 100 m, 1000 m, and seabed flux estimates, as well as sediment burial estimates, all agree well, especially south of the APF. Even though some of the export estimates were made over very different time scales, the overall trend is very clear, and supported by all flux estimates.

Conditions within and north of the APF can help to explain some of the discrepancies between the ^{234}Th fluxes and the other flux estimates. The Antarctic Polar Front is an area of elevated horizontal and vertical velocities, relative to areas to the north and south (Barth et al. in press). Therefore, the physics of the APF could have resulted in much more flux out of the upper 100 m, as evidenced by ^{234}Th fluxes, than could be measured as net Si removal or sedimentation to 1,000 m. Specifically, the highly energetic APF zone would have higher rates of $Si(OH)_4$ resupply through mixing and upwelling, as was observed in December, and the higher current velocities would also transport sinking material much farther than less energetic areas to the north and south. Therefore it is possible that the 50 m and 1,000 m flux estimates missed significant amounts of $BSiO_2$ export in the APF the. Additionally, the assumption that sediment trap fluxes are similar interannually may be invalid, and the low flux to 1,000 m in the APF zone could simply be due to sampling during a different year.

Furthermore, given that the APF and areas to the north are permanently ice-free, diatom production is likely to begin earlier and last longer than in areas that are seasonally ice covered. Therefore, significant amounts of $BSiO_2$ production and export could occur that were not directly measured as changes in total Si. It is thus likely that

the 50 m export estimates in the sub-Antarctic and APF zones significantly underestimate annual export due to periods of export outside the November to March sampling period. More specifically, initial total Si in the upper 50 m (as determined during the November cruise) was likely an underestimate of total Si at the beginning of the growing season within and north of the APF, and therefore caused the seasonal $Si(OH)_4$ removal, and hence export, to be underestimated. The underestimation of 50 m $BSiO_2$ export would be most prominent in the sub-Antarctic zone, where $[Si(OH)_4]$ was already <10 mmol m^{-3} in November.

$BSiO_2$ flux to 1,000 m was between 40 and 45% of our 50 m Si export estimates, except for the northernmost sub-Antarctic zone (Table 5). In the sub-Antarctic region, sediment trap flux estimates were 89% of our estimated $BSiO_2$ export from the surface layer. This percentage of export caught in sediment traps is very high for open ocean systems, and may simply reflect the fact that most of the sediment trap data were from the previous year. Additionally, the likely underestimation of annual 50 m export would certainly create the appearance of an unusually high percentage of 50 m export reaching 1,000 m (see above). Other than the underestimate of 50 m export in the sub-Antarctic region, export based on net changes in Si compare very well with sediment trap fluxes to 1,000 m, accumulation at the seafloor, and burial in the sediments. Based on these estimates, an average of >40% of the $BSiO_2$ exported from the upper 50 m reaches 1,000 m and 50% of the 50 m export reaches the seafloor. These findings imply rapid sinking of diatom particulate matter throughout the water column, with essentially 100% preservation of sinking $BSiO_2$ between 1,000 m and the seafloor.

Based on the 50 m export and sediment burial rates (Table 5), burial efficiency estimates, defined as the % of 50 m export that is buried, were calculated. An average of 5.3% of Si exported from the upper 50 m is buried in sediments beneath the Southern Ocean along 170° W between 58° and 68° S. The southern ACC zone had the highest burial efficiency at 7.7% and the Ross Sea Gyre zone had the lowest at 3.1%. This estimate of burial efficiency beneath the southern ACC along 170° W is very similar to the 9.1% burial efficiency estimated by Pondaven et al. (2000) for the region south of the APF in the Indian sector of the Southern Ocean. Therefore, the hydrographic region just

south of the APF supports very similar Si flux out of the surface layer, as well as burial in the deep sea sediments, in different areas of the Southern Ocean.

The region south of the APF has the highest $Si(OH)_4$ removal, the highest $BSiO_2$ concentrations, and the highest sediment accumulation and burial of $BSiO_2$ in both the Pacific and Indian sectors of the Southern Ocean. Furthermore, these burial efficiencies are only slightly higher than the global average of 5%, whereas the estimates of $BSiO_2$ production, based net removal of $Si(OH)_4$, in this region are 6-7 times higher than the global average (Tréguer et al. 1995). This analysis indicates that although $BSiO_2$ preservation is slightly higher than the global mean in some areas of the Southern Ocean, it is the extremely high production and flux of $BSiO_2$ that is likely responsible for the accumulation of opal sediments beneath the ACC.

High diatom biomass develops only in regions of high initial $[Si(OH)_4]$, and is therefore limited to waters south of the APF. Apparently, high concentrations of $BSiO_2$ in the open Southern Ocean along 170° W are also limited to waters north of the SACCF, at ~65°S. North of 61° S the available $Si(OH)_4$ is exported efficiently, but the initial standing stock of Si limits production and therefore export. The fact that high $[Si(OH)_4]$ occur south of 65° S throughout the study period indicates that other factors, such as a short growing season, limit diatom production, resulting in low annual $BSiO_2$ export that amounts to only a small fraction of the available Si. The region between the APF and the SACCF also experiences large seasonal variations in mixed layer depths, due to the stabilizing influence of melt water from the receding sea ice, at least in the Pacific sector. Mixed layers in this region shoaled from >100 m in November to <30 m in December and January. The shallower mixed layers in December and January were likely instrumental in the high accumulation of $BSiO_2$. This is supported by the fact that vertical gradients in $[Si(OH)_4]$ were not present in the upper 80 m in November, but became very steep and shallow by January. Therefore, this region of the Southern Ocean promotes high diatom accumulation in the surface layer, via the high initial $[Si(OH)_4]$ and the shallow, stabilized melt water lens. What is obvious is that the region of the ACC between the APF and the SACCF supports higher fluxes of $BSiO_2$ out of the surface layer, to 1000 m and the seabed, as well as Si burial rates, than any other open ocean system. Thus, a robust interpretation of the data presented here is that the very high flux

of diatom $BSiO_2$ from the surface layer, and not high burial efficiency, is responsible for the high burial rates of Si in Southern Ocean sediments, as compared to abyssal sediments in other oceanic environments. Specifically, it is the co-occurrence of high winter $[Si(OH)_4]$, high $BSiO_2$ production, and efficient export of the $BSiO_2$ that is unique to the southern ACC of the Southern Ocean. This combination of factors does not occur in other marine systems, and appears to be the primary cause of the vast opal belt surrounding Antarctica.

Bibliography

Alldredge, A.L. and C. D. Gotschalk. 1988. *In situ* settling behavior of marine snow. Limnol. & Oceanogr. 33: 339-351.

Antoine, D., J-M. André, and A. Morel. 1996. Oceanic primary production 2. Estimation at global scale from satellite (coastal zone color scanner) chlorophyll. Glob. Biogeochem. Cycl. 10: 57-69.

Banse, K. 1982. Cell volumes, maximal growth rates of unicellular algae and ciliates, and the role of ciliates in the marine pelagial. Limnol. Oceanogr. 27: 1059-1071.

Barth, J.A., T.J. Cowles, and S.D. Pierce. (in press). Mesoscale physical and bio-optical structure of the Antarctic Polar Front near 170°W during spring. J. Geophys. Res.

Belkin, I.M. and A.L. Gordon. 1996. Southern Ocean fronts from the Greenwhich meridian to Tasmania. J. Geophys. Res. 101: 3675-3696.

Billet, D.S.M., R.S. Lampitt, A.L. Rice, and R.F.C. Mantoura. 1983. Seasonal sedimentation of phytoplankton to the deep sea benthos. Nature 302: 520-522.

Brainerd, K.E. and M.C. Gregg. 1995. Surface mixed and mixing layer depths. Deep-Sea Res. 42: 1521-1543.

Brzezinski, M.A. 1985. The Si:C:N ratio of marine diatoms. Interspecific variability - and the effect of some environmental variables. J. Phycol. 21: 347-357.

Brzezinski, M.A. and D.M. Nelson. 1989. Seasonal changes in the silicon cycle within a Gulf Stream warm-core ring. Deep-Sea Res. 36: 1009-1030.

Brzezinski, M.A., R.J. Olson, and S.W. Chisholm. 1990. Silicon availability and cell-cycle progression in marine diatoms. Mar. Ecol. Progr. Ser. 67: 83-96.

Brzezinski, M.A. and D.M. Nelson. 1996. Chronic substrate limitation of silica production in the Sargasso Sea. Deep-Sea Res. (II) 43: 437-453.

Brzezinski, M.A. and D.R. Phillips. 1997. Evaluation of 32Si as a tracer for measuring silica production rates in marine waters. Limnol. Oceanogr. 42: 856-865.

Brzezinski, M.A., D.M. Nelson, V.M. Franck, and D.E. Sigmon. (in press). Silicon dynamics within an intense open-ocean diatom bloom in the Pacific sector of the Southern Ocean. Deep-Sea Res. (II).

Buesseler, K.O. 1998. The decoupling of production and particulate export in the surface ocean. Glob. Biogeochem. Cycl. 12: 297-310.

Buesseler, K.O., L. Ball, J. Andrews, J.K. Cochran, D.J. Hirschberg, M.P. Bacon, A. Fleer, and M.A. Brzezinski. (in press). Upper ocean export of particulate organic carbon and biogenic silica in the Southern Ocean along 170°W. Deep-Sea Res. (II).

Comiso, J.C., C.R. McClain, C.W. Sullivan, J.P. Ryan, and C.L. Leonard. 1993. Coastal zone color scanner pigment concentrations in the Southern Ocean and relationship to geophysical surface features. J. Geophys. Res. 98: 2,419-2,451.

DeMaster, D.J. 1981. The supply and accumulation of silica in the marine environment. Geochim. Cosmochim. Acta 45: 1715-1732.

DeMaster, D.J., R.B. Dunbar, L.I. Gordon, A.R. Leventer, J.M. Morrison, D.M. Nelson, C.A. Nittrouer and W.O. Smith, Jr. 1992. The cycling and accumulation of organic matter and biogenic silica in high-latitude environments: The Ross Sea. Oceanogr. 5: 146-153.

DeMaster, D.J., W.O. Smith, D.M. Nelson, and J.Y. Aller. 1996. Biogeochemical processes in Amazon shelf waters: chemical distributions and uptake rates of silicon, carbon, and nitrogen. Continent. Shelf Res. 16: 617-643.

DeMaster, D.J. Submitted. Continental margin biogenic silica accumulation: coupling of the marine cycles of organic matter and biogenic silica. Deep-Sea Res.

Fortier, L., J. Le Fevre, and L. Legendre. 1994. Export of biogenic carbon to fish deep ocean: the role of large planktonic microphages. J. Plankton Res. 16: 809-839.

Froneman, P.W. and R. Perissinitto. 1996. Microzooplankton grazing and protozooplankton community structure in the South Atlantic and in the Atlantic sector of the Southern Ocean. Deep-Sea Res. 43: 703-721.

Frost, B.W. 1991. The role of grazing in nutrient-rich areas of the open sea. Limnol. Oceanogr. 36: 1616-1630.

Furnas, M. 1990. In situ growth rates of marine phytoplankton: approaches to measurement, community and species growth rates. J. Plankton Res. 12: 1117-1151.

Gordon, A.L. 1967. Structure of Antarctic waters between 20°W and 170°W. Antarct. Map Foli Ser., folio 6, (V.C. Bushnell, ed.). Am. Geogr. Soc., New York. 10 pp.

Harrison, P.J., H.L. Conway, R.W. Holmes, and C.O. Davis. 1977. Marine diatoms grown in chemostats under silicate or ammonium limitation. III. Chemical composition and morphology of *Chaetoceros debilis*, *Skeletonema costatum*, and *Thalassiosira gravida*. Mar. Bio. 43: 19-31.

Honjo. S, R. Collier, R. Francois, S. Manganini, and J. Dymond. 2000. Particle fluxes to the interior of the Southern Ocean in the western Pacific sector along 170°W. Deep-Sea Res. (II) 42(15-16): 3,521-3,548.

Jennings, J.C., Jr., L.I. Gordon, and D.M. Nelson. 1984. Nutrient depletion indicates high primary productivity in the Weddell Sea. Nature 308: 51-54.

Komar, P.D., A.P. Morse, and L.F. Small. 1981. An analysis of sinking rates of natural copepod and euphausid fecal pellets. Limnol. Oceanogr. 26: 172-180.

Lampitt, R.S. 1985. Evidence for the seasonal deposition of detritus to the deep-sea floor and its subsequent resuspension. Deep-Sea Res. 32: 885-897.

Legendre, L. and J. Le Fevre. 1995. Microbial food webs and the export of biogenic carbon in the oceans. Aquat. Microb. Ecol. 9: 69-77.

LeJehan, S. and P. Tréguer. 1983. Uptake and regeneration Si/ N/ P ratios in the Indian sector of the Southern Ocean: Originality of the biological cycle of silicon. Polar Bio. 2: 127-136.

Lisitzin, A.P. 1972. Sedimentation in the world ocean. Banda press, Tulsa, OK, 218 pp.

Lutjeharms, J.R.E., N.M. Walters, and B.R. Allanson. 1985. Oceanic frontal systems and biological enhancement. In: Antarctic nutrient cycles and food webs (W.R. Siegfried, P.R. Condy and R.M. Laws, eds.) Springer-Verlag, pp. 11-21.

Michaels, A.F. and M.W. Silver. 1988. Primary production, sinking fluxes and the microbial food web. Deep-Sea Res. 35: 473-490.

Moore, J.K., M.R. Abbott, and J.G. Richman. 1999. Location and dynamics of the Antarctic Polar Front from satellite sea surface temperature data. J. Geophys. Res. 104: 3,059-3,073.

Nelson, D.M. and J.J. Goering. 1977b. Near-surface silica dissolution in the upwelling region off northwest Africa. Deep-Sea Res. 24: 65-73.

Nelson, D.M., J.J. Goering, and D.W. Boisseau. 1981. Consumption and regeneration of silicic acid in three coastal upwelling systems. In: Coastal upwelling (F.A. Richards, ed.), American Geophysical Union, Washington, D.C., pp. 242-256.

Nelson, D.M., W.O. Smith, Jr., L.I. Gordon, and B.A. Huber. 1987. Spring distributions of density, nutrients and phytoplankton biomass in the ice-edge zone of the Weddell-Scotia Sea. J. Geophys. Res. 92: 7,181-7,190.

Nelson, D.M., P. Tréguer, M.A. Brzezinski, A. Leynaert, and B. Quéguiner. 1995. Production and dissolution of biogenic silica in the ocean: Revised global estimates,

comparison with regional data and relationship to biogenic sedimentation. Glob. Biogeochem. Cycl. 9: 359-372.

Nelson, D.M. and Q. Dortch. 1996. Silicic acid depletion and silicon limitation in the plume of the Mississippi River: evidence from kinetic studies in spring and summer. Mar. Ecol. Progr. Ser. 136: 163-178.

Nelson, D.M. and M.A. Brzezinski. 1997. Diatom growth and productivity in an oligotrophic midocean gyre: A 3-yr record from the Sargasso Sea near Bermuda. Limnol. Oceanogr. 42: 473-486.

Nelson, D.M., M.A. Brzezinski, D.E. Sigmon, and V.M. Franck. (in press). A seasonal progression of Si limitation in the Pacific sector of the Southern Ocean. Deep-Sea Res. (II).

Nelson, D.M., R.F. Anderson, R.T. Barber, M.A. Brzezinski, K.O. Buesseler, Z.Chase, R.W. Collier, M. Dickson, R. François, M.R. Hiscock, S. Honjo, J. Marra, W.R. Martin, R.N. Sambrotto, F.L. Sayles, and D.E. Sigmon. (in press). Vertical budgets for organic carbon and biogenic silica in the Pacific sector of the Southern Ocean, 1996-1998. Deep-Sea Res. (II).

Parsons, T.R., M. Takahasi, and B. Hargrave. 1984. Biological oceanographic processes. Pergammon Press, Oxford, 330 pp.

Pondaven, P., O. Ragueneau, P. Treguer, A. Hauvespre, L. Dezileau, and J.L. Reyss. 2000. Resolving the 'opal paradox' in the Southern Ocean. Nature 405: 168-172.

Sayles, F.L., W.R. Martin, Z. Chase, and R.F. Anderson. (in press). Benthic remineralization and burial of biogenic SiO_2, $CaCO_3$, and organic carbon and detrital material in the Southern Ocean along a transect at 170W. Deep-Sea Res. II.

Smayda, T.J. 1990. Novel and nuisance phytoplankton blooms in the sea: Evidence for a global epidemic. p. 29-40 In: Toxic marine phytoplankton. (E. Granelli, B Sundstrom, R. Edler, and D.M. Anderson, eds) Elsevier, New York, pp. 29-40.

Smetacek, V. 1985. Role of sinking in diatom life-history cycles: ecological, evolutionary and geological significance. Mar. Bio. 84: 239-251.

Strickland, J. D. H. and T. R. Parsons. 1972. A Practical Handbook of Seawater Analysis. Fish. Res. Bd. Can. Bull. 167. 2nd ed. pp. 65-70.

Stumm, W. and J.J. Morgan. 1981. Aquatic chemistry, 2nd ed., Wiley, New York. 780 pp.

Tang, Y. 1995. The allometry of algal growth rates. J. Plankton Res. 17: 1325-1335.

Townsend, D.W., M.D. Keller, M.E. Sieracki, and S.G. Ackleson. 1992. Spring phytoplankton blooms in the absence of vertical water column stratification. Nature 360: 59-62.

Townsend, D.W., L.M. Cammen, P.M. Holligan, D.E. Campbell, and N.R. Pettigrew. 1994. Causes and consequences of variability in the timing of spring phytoplankton blooms. Deep-Sea Res. 41: 747-765.

Tréguer, P., D.M. Nelson, A.J. van Bennekom, D.J. DeMaster, A. Leynaert, and B. Quéguiner. 1995. The silica balance in the world ocean: A re-estimate. Science 268: 375-379.

van Bennekom, A.J., G.W. Berger, S.J. van der Gaast, R.T.P. de Vries. 1988. Primary productivity and the silica in the Southern Ocean (Atlantic sector). In: The polar ocean: the Antarctic: present and past, E. Olansson (ed.). Palaeogeogr. Palaeoclimatol., Palaeoecol., Spec. Issue 66: 19-30.

Appendix

Appendix

This appendix is a listing of the original station profile data collected between October 1997 and March 1998 that was used to construct the 50 m Si budget described in this thesis. Data for each station consists of 8 discrete samples collected at the 85% (shallowest depth), 50%, 25%, 18%, 10%, 5%, 1%, and 0.1% (deepest depth) light depth as described in the methods section of Chapter 2. Only the actual depth of each discrete sample is shown.

Station	Sampling Date	Latitude (°S)	Longitude (°W)	Depth (m)	$[Si(OH)_4)]$ (mmol m^{-3})	$BSiO_2$ (mmol m^{-3})
Survey 1						
3	Oct. 30	62.37	170.08	2.8	46.57	0.96
				12.2	46.51	0.98
				25.3	46.38	1.00
				31.5	46.51	0.97
				42.0	46.64	0.98
				54.9	46.00	1.28
				88.7	47.41	0.98
				132.9	48.40	0.87
8	Nov. 3	60.50	169.00	3.8	27.37	0.84
				12.1	27.41	0.82
				27.8	27.37	0.77
				34.5	27.25	0.75
				43.1	27.33	0.91
				57.3	27.13	0.98
				89.0	27.09	0.83
				135.7	26.89	0.57
12	Nov. 6	59.33	170.00	3.0	15.27	0.42
				12.7	15.27	0.40
				26.0	15.42	0.40
				32.9	15.30	0.46
				44.5	15.33	0.40
				59.2	15.36	0.39
				87.8	15.72	0.40
				133.6	16.22	0.38
16	Nov. 9	59.96	171.90	11.3	15.31	0.37
				21.3	15.31	0.40
				41.6	15.31	0.54
				50.5	15.31	0.36
				62.5	15.31	0.39
				102.9	15.19	0.38
				131.9	15.43	0.40
				162.4	15.43	0.41

Station	Sampling Date	Latitude (°S)	Longitude (°W)	Depth (m)	$[Si(OH)_4)]$ (mmol m^{-3})	$BSiO_2$ (mmol m^{-3})
18	Nov. 15	60.24	170.69	3.4	17.08	0.38
				14.2	17.20	0.40
				26.2	17.08	0.37
				31.6	17.20	0.41
				43.0	17.01	0.37
				54.3	17.01	0.41
				84.7	16.83	0.51
				128.4	17.14	0.39
23	Nov. 20	60.83	168.29	3.5	28.40	1.27
				9.0	28.40	1.22
				17.4	28.40	1.10
				21.6	28.49	1.18
				28.7	28.16	1.18
				37.9	28.32	1.41
				59.0	28.00	1.28
				89.4	28.49	1.28
Process 1						
1	Dec. 7	53.03	174.70	2	1.08	1.52
				11	1.12	1.42
				21	0.89	1.81
				26	0.57	2.05
				35	0.51	2.09
				46	0.84	1.94
				70	1.66	1.66
				105	2.93	0.89
2	Dec. 9	56.84	170.16	4	7.55	0.30
				17	7.50	0.32
				34	7.65	0.32
				42	7.85	0.40
				56	7.82	0.32
				73	8.02	0.25
				112	8.23	0.17
				167	9.80	0.09
3	Dec. 10	58.50	170.00	5	7.63	2.24
				10	7.58	2.20
				20	7.69	2.23
				30	7.23	2.55
				40	7.76	2.71
				50	9.61	2.42
				60	12.13	2.39
				70	12.30	0.63

Station	Sampling Date	Latitude (°S)	Longitude (°W)	Depth (m)	$[Si(OH)_4)]$ (mmol m^{-3})	$BSiO_2$ (mmol m^{-3})
4	Dec. 13	60.23	170.07	2	5.06	4.99
				6	5.07	4.88
				12	5.03	4.91
				14	5.06	4.63
				19	5.75	4.65
				25	6.31	4.49
				39	12.50	0.84
				63	15.14	3.88
5	Dec. 14	60.92	169.25	2	13.63	4.04
				9	16.31	4.67
				18	19.83	4.27
				23	18.48	7.46
				31	17.89	6.66
				40	17.90	10.50
				61	28.74	2.06
				92	33.68	1.08
6	Dec. 16	61.67	168.83	1	31.51	8.50
				6	31.56	8.77
				12	31.60	8.66
				15	32.32	7.96
				20	32.73	7.69
				26	34.79	10.04
				39	46.02	5.77
				50	50.25	1.00
7	Dec. 19	64.15	169.19	1	53.91	7.12
				5	53.51	7.12
				10	53.75	7.16
				12	53.51	6.24
				16	54.14	6.22
				21	57.14	7.76
				32	64.29	3.58
				49	68.44	0.95
8	Dec. 20	64.70	169.29	1	46.15	7.44
				5	45.93	7.53
				9	46.15	7.69
				12	43.78	7.95
				15	43.78	7.79
				20	46.00	8.64
				31	56.94	3.39
				46	62.21	1.00

Station	Sampling Date	Latitude (°S)	Longitude (°W)	Depth (m)	$[Si(OH)_4)]$ (mmol m^{-3})	$BSiO_2$ (mmol m^{-3})
9	Dec. 21	63.09	169.85	5	24.38	10.57
				10	32.27	10.62
				12	36.01	9.26
				16	34.84	9.24
				21	35.96	7.80
				33	49.97	3.63
				49	53.13	0.99
10	Dec. 24	62.40	169.83	1	13.52	12.40
				5	13.40	11.91
				10	13.32	12.43
				13	13.40	12.87
				17	13.49	12.51
				22	13.58	12.65
				34	17.03	11.23
				51	29.25	10.62
11	Dec. 25	61.67	168.83	6.2	14.40	11.27
				11.0	14.40	10.42
				21.9	14.30	11.31
				31.6	15.60	11.96
				41.3	19.70	13.19
				50.6	30.90	10.24
				61.4	36.20	8.28
				71.0	39.90	5.31
				82.2	43.60	3.58
12	Dec. 25	61.17	168.83	4.0	23.10	7.12
				10.1	23.10	6.11
				20.1	23.00	6.93
				30.8	23.40	7.06
				40.2	24.00	7.03
				49.8	23.80	7.15
				59.7	29.20	6.65
				71.0	33.50	4.74
				81.4	36.70	4.68
13	Dec. 25	60.67	168.83	10.3	11.80	4.89
				22.7	11.60	4.81
				32.9	11.80	4.81
				42.5	12.00	4.66
				52.3	12.20	4.94
				61.7	12.80	4.57
				71.2	14.10	4.06
				81.9	20.10	1.83

Station	Sampling Date	Latitude (°S)	Longitude (°W)	Depth (m)	$[Si(OH)_4)]$ (mmol m^{-3})	$BSiO_2$ (mmol m^{-3})
14	Dec. 25	60.79	168.83	11.6	8.40	8.47
				16.2	8.10	8.37
				27.3	10.60	7.42
				36.2	18.50	2.49
				46.1	20.20	2.24
				57.6	21.50	1.74
				66.9	24.00	1.20
				77.8	24.60	1.08
				86.2	24.60	1.03
15	Dec. 25	60.92	169.83	8.6	13.90	5.32
				16.2	13.70	5.62
				27.0	13.90	6.35
				34.7	13.60	5.68
				45.7	13.30	6.30
				55.8	13.70	5.83
				66.2	24.80	5.54
				75.7	28.10	1.52
				85.4	27.70	1.33
16	Dec. 26	61.04	168.83	5.2	17.50	6.18
				11.1	17.50	6.29
				20.8	17.50	7.32
				31.0	17.70	7.51
				41.2	17.90	7.48
				51.7	19.30	8.30
				62.1	23.30	6.76
				71.9	28.20	5.19
				80.2	35.30	3.07
17	Dec. 28	55.66	171.74	2	4.97	1.71
				10	4.90	1.61
				21	4.97	1.66
				26	4.80	1.78
				35	4.90	1.66
				45	4.92	1.64
				69	6.40	1.69
18	Dec. 30	54.33	173.33	1	0.32	3.62
				6	0.31	3.73
				13	0.33	3.52
				15	0.33	3.89
				21	0.39	3.87
				27	0.38	3.86
				42	0.49	3.71
				62	0.73	3.58

Station	Sampling Date	Latitude (°S)	Longitude (°W)	Depth (m)	$[Si(OH)_4)]$ (mmol m^{-3})	$BSiO_2$ (mmol m^{-3})
19	Dec. 31	52.98	174.62	2	0.26	0.80
				11	0.26	0.85
				21	0.27	0.78
				26	0.28	0.78
				35	0.27	0.70
				46	0.30	0.68
				70	0.50	1.01
				105	2.03	0.56
Survey 2						
3	Jan. 17	67.78	170.11	2	60.91	3.82
				10	61.17	3.82
				20	60.91	3.82
				24	64.87	4.53
				34	64.87	3.53
				44	67.16	1.10
				67	70.28	0.60
				101	70.48	0.45
4	Jan. 20	64.83	170.10	4	17.86	16.568
				8	17.96	16.934
				10	17.81	15.815
				14	17.96	16.796
				18	17.96	17.930
				27	18.11	17.166
				41	49.85	10.734
5	Jan. 21	62.00	170.10	3	4.60	5.740
				7	4.60	4.862
				10	5.14	6.976
				13	miss fire	2.442
				17	4.51	5.165
				23	4.55	7.133
				35	4.56	7.107
				49	5.00	6.461
6	Jan. 27	60.00	170.10	3	2.08	0.693
				12	2.04	0.859
				24	2.09	0.877
				30	2.04	0.918
				40	2.02	0.569
				52	10.66	1.333
				79	12.81	0.216
				119	14.66	0.739

Station	Sampling Date	Latitude (°S)	Longitude (°W)	Depth (m)	$[Si(OH)_4)]$ (mmol m^{-3})	$BSiO_2$ (mmol m^{-3})
7	Jan. 28	61.00	170.10	4	2.32	1.231
				13	2.30	2.295
				26	2.33	-0.008
				32	2.47	1.525
				43	2.45	1.451
				56	4.74	2.006
				85	23.22	1.032
				128	27.39	1.023
8	Jan. 29	65.17	170.10	3	24.93	12.061
				6	25.08	10.653
				12	25.46	12.413
				16	24.89	12.956
				22	25.96	18.528
				28	28.37	3.017
				42	60.60	3.100
				59	71.00	0.734
Process 2						
1	Feb. 18	52.97	174.73	2	1.11	0.28
				11	0.96	0.32
				21	0.95	0.31
				26	0.93	0.29
				35	0.94	0.30
				46	0.92	0.29
				70	1.33	0.19
				105	2.72	0.11
2	Feb. 20	56.85	170.17	3	2.04	0.78
				13	2.03	1.04
				26	2.01	1.05
				32	1.99	1.01
				43	2.02	1.22
				55	1.97	1.27
				85	2.78	1.66
				128	10.19	0.31
4	Feb. 23	60.23	170.07	4	6.66	0.37
				15	6.61	0.35
				30	6.71	0.36
				37	6.71	0.55
				50	6.64	0.52
				65	6.71	0.39
				100	16.00	0.29
				150	18.62	0.54

Station	Sampling Date	Latitude (°S)	Longitude (°W)	Depth (m)	$[Si(OH)_4)]$ (mmol m^{-3})	$BSiO_2$ (mmol m^{-3})
7	Feb. 26	63.08	169.88	3	13.33	1.32
				12	13.36	1.53
				25	13.31	1.31
				31	13.33	1.40
				41	13.39	1.35
				53	22.43	1.85
				82	58.85	1.32
				123	61.57	0.76
9	Mar. 1	66.10	168.67	2	53.43	3.52
				56*	64.16	2.79
				20	53.13	3.67
				25	52.98	3.73
				34	52.91	3.43
				44	53.96	2.76
				68	74.51	1.14
				102	75.96	0.40
13	Mar. 4	70.40	165.91	2	57.09	5.22
				8	57.09	4.67
				16	57.18	4.17
				20	58.00	4.54
				27	58.00	4.56
				35	58.33	4.71
				54	69.72	2.35
				81	71.59	0.45
14	Mar. 6	71.31	165.96	2	49.40	5.40
				8	48.86	5.29
				15	48.99	5.61
				19	49.13	5.71
				25	49.20	5.96
				33	49.40	5.75
				50	62.48	0.64
				75	66.02	2.46
15	Mar. 7	69.30	168.37	2	60.02	1.00
				11	59.94	0.96
				21	59.76	0.98
				26	59.76	1.07
				35	61.77	1.21
				46	67.70	0.70
				70	68.75	0.27
				105	71.67	0.22

Station	Sampling Date	Latitude (°S)	Longitude (°W)	Depth (m)	$[Si(OH)_4)]$ (mmol m^{-3})	$BSiO_2$ (mmol m^{-3})
16	Mar. 8	67.50	170.00	3	60.86	1.40
				12	60.86	1.38
				24	61.03	1.45
				30	61.12	1.25
				40	60.60	1.27
				52	67.30	1.29
				80	73.57	0.43
				120	83.00	0.22
18	Mar. 10	64.70	169.33	3	20.44	0.95
				13	20.37	0.97
				20	20.34	0.95
				32	20.44	1.18
				43	20.51	1.20
				56	49.64	1.03
				86	61.73	0.90
				129	67.34	0.66
20	Mar. 12	61.67	170.10	4	9.98	0.50
				15	10.06	0.50
				30	10.01	0.49
				38	9.98	0.53
				51	10.04	0.52
				66	10.23	0.62
				101	41.42	0.59
				152	47.33	0.48
26	Mar. 14	60.23	170.10	4	5.72	0.28
				16	7.77	0.43
				32	5.68	0.35
				39	5.68	0.05
				53	5.75	0.15
				69	6.07	0.17
				106	11.65	0.18
				159	20.64	0.24
27	Mar. 14	58.50	170.00	4	4.53	0.13
				17	4.47	0.15
				33	4.54	0.16
				41	4.55	0.12
				55	4.56	0.14
				72	4.67	0.14
				110	13.36	0.16
				165	18.66	0.38

Station	Sampling Date	Latitude (°S)	Longitude (°W)	Depth (m)	$[Si(OH)_4)]$ (mmol m^{-3})	$BSiO_2$ (mmol m^{-3})
29	Mar. 16	54.33	173.33	6	2.16	No sample
				15	2.20	0.06
				30	2.13	0.06
				49	2.15	0.06
				63	2.26	0.06
				98	3.00	0.09
				145	7.51	0.16